ARTICLE OPEN

Check for updates

Upregulation of CCK3R leading to the suppression of chronic seizures

Ling He[1,2,3,4,5]✉, Liyang Zhang[1,2,3,4,5], Yujie Yang[1,2,3,4,5], Junming Ren[1,2,3,4], Zhoujian Xiao[1,2,3,4], Yihao Li[1,2,3,4], Yuandi Zhao[1,2,3,4], Feixu Jiang[1,2,3,4], Dingxuan Zeng[1,2,3,4], Xin Yan[1,2,3,4], Yanyan Sun[1,2,3,4] and Jufang He[1,2,3,4]✉

Epilepsy is a chronic neurological disorder characterized by recurrent seizures that affect millions globally. Despite the availability of various antiepileptic drugs, 30–40% of patients remain drug-resistant and continue to experience seizures. This unmet need has driven the search for novel therapies, including gene therapy. This study aimed to explore G protein-coupled receptor 173 (GPR173), also referred to as cholecystokinin receptor 3, as a gene therapy strategy for epilepsy. Previous research suggests that the upregulation of GPR173 might benefit epilepsy treatment by modulating the gamma-aminobutyric acid cholecystokinin signaling pathway involved in inducing inhibitory long-term potentiation. In a mouse model of kainic acid-induced epilepsy, GPR173 overexpression, controlled by either the cytomegalovirus or calcium/calmodulin-dependent protein kinase II promoter, significantly reduced spontaneous seizures in chronic epileptic mice. Notably, specific upregulation of GPR173 in excitatory neurons led to a more pronounced seizure reduction than in controls. Importantly, this gene therapy does not appear to cause severe adverse effects on physiological functions such as locomotor activity, anxiety, and spatial memory. However, the overexpression of GPR173 may affect the appetite of animals, thereby slowing down normal weight gain. Overall, these findings highlight the therapeutic potential of GPR173 in seizure suppression and suggest it as a new promising candidate target for epilepsy treatment.

Translational Psychiatry (2025)15:457 ; https://doi.org/10.1038/s41398-025-03680-1

INTRODUCTION

Epilepsy, or seizure disorder, is a neurological disease characterized by transient motor, sensory, psychiatric, autonomic, and visual signs and symptoms. It leads to an increased predisposition of the brain to generate seizures and is often accompanied by cognitive and psychosocial decline [1]. The manifestation and recurrence of seizures vary considerably among individuals diagnosed with epilepsy, ranging from momentary attentional deficits to severe convulsive episodes. Although the precise etiology of epilepsy often remains undetermined, various factors, including cerebral trauma, genetic susceptibility, and neurodevelopmental abnormalities, may contribute to its emergence. Hyperexcitability and hypersynchronous firing of neurons, caused by an imbalance between neuronal excitation and inhibition (E/I), drive seizure initiation in one or more brain subcortical or cortical circuits. The extent of seizure propagation within a local or remote epileptic network ultimately determines its severity and impact on behavior [2].

Globally, epilepsy affects approximately 0.5–1% of the human population [3], and many of these patients are refractory to currently available antiepileptic drugs (AEDs) [4–6]. Unrestrained excitability and loss of gamma-aminobutyric acid (GABAergic) inhibitory control are prerequisites for seizure initiation and propagation [2, 7]; these provide the basis for developing AEDs that either reduce excitation or increase inhibition. Studies have reported the involvement of GABAergic inhibitory circuits in the formation, propagation, and treatment of central nervous system (CNS) disorders, including epilepsy [8–10]. Numerous pharmaceuticals, including benzodiazepines, have been developed or are currently being developed by targeting GABA-related mechanisms for epilepsy treatment [10, 11]. Nevertheless, potential limitations of these direct GABA-targeted drugs result in several unavoidable adverse effects, partially attributable to the extensive distribution and indispensable functions of GABA receptors [12]. Despite the availability of various antiepileptic drugs, 30–40% of patients remain drug-resistant and continue to experience seizures, highlighting a significant unmet medical need. This persistent challenge underscores the urgent necessity for novel therapeutic approaches to address drug-resistant epilepsy. Researchers are actively exploring alternative treatment modalities, including neuromodulation techniques and targeted gene therapies, to improve seizure control [13, 14]. Considering the challenges associated with tolerability, safety, and therapeutic efficacy of several AEDs, current and future epilepsy treatment research is focused on novel therapeutic approaches with new targets.

Seizures involve the widespread recruitment of neurons across multiple cortical and subcortical brain areas, forming a broad epileptogenic network. Therefore, a treatment approach targeting

[1]Department of Neuroscience, City University of Hong Kong, Kowloon, Hong Kong. [2]Department of Biomedical Science, City University of Hong Kong, Kowloon, Hong Kong. [3]Research Institute of City University of Hong Kong, Shenzhen 518057, China. [4]Center of Regenerative Medicine and Health, Hong Kong Institute of Science and Innovation, Chinese Academy of Sciences, Hong Kong, Hong Kong. [5]These authors contributed equally: Ling He, Liyang Zhang, Yujie Yang. ✉email: linghe5@cityu.edu.hk; jufanghe@cityu.edu.hk

Received: 29 August 2024 Revised: 9 September 2025 Accepted: 2 October 2025
Published online: 31 October 2025

the entire network, rather than solely the seizure focus, is likely to be more effective in suppressing epileptic seizures. Gene therapy offers a strategy for the knockdown or overexpression of specific genes within large-scale pathological networks by incorporating genes into adeno-associated virus (AAV) [15, 16]. This therapeutic approach has been proposed to treat neurological disorders such as Parkinson's, Alzheimer's, and Huntington's diseases [17–19]. Furthermore, gene therapy is also being explored for its potential benefits in epilepsy treatment [13, 14].

G protein-coupled receptor 173 (GPR173), also known as super conserved receptor expressed in the brain, belongs to a highly evolutionary conserved and predominantly expressed receptor family in the CNS [20]. Initially identified as an orphan receptor, GPR173 plays crucial roles in various physiological processes. Researchers discovered that GPR173 mediates the action of Phoenixin by activating the cAMP-PKA pathway, which induces gene expression related to reproductive functions [21]. Furthermore, metabolic factors can regulate the expression of GPR173 through a p38-mediated mechanism, indicating that GPR173 may influence metabolic diseases, such as obesity and diabetes, by affecting metabolic pathways and responses to dietary components [22]. Additionally, GPR173 plays a vital role in bone metabolism and inflammatory response regulation. Activation by its agonist Phoenixin-20 not only promotes osteoblastic differentiation, essential for bone formation and homeostasis [23] but also reduces lipopolysaccharide-induced cytotoxicity and decreases inflammatory cytokine expression [24]. These findings suggest that GPR173 may serve as different mediators depending on the pathway in which it is involved.

Long-term potentiation (LTP), a form of synaptic plasticity, induces a long-lasting enhancement in synaptic strength following high-frequency stimulation of a synapse [25]. LTP in inhibitory synapses (iLTP) [25, 26], strengthens inhibitory neurotransmission, synergistically working with excitatory LTP to maintain the E/I balance within neural circuits [27, 28]. Our prior work identified GPR173 as a novel CCK receptor (CCK3R) mediating iLTP induction, thereby enhancing GABAergic inhibition onto neocortical pyramidal neurons [29]. Given that up to 15–20% of neocortical neurons are inhibitory GABAergic neurons [30] crucial for maintaining E/I balance of the cortex [31, 32], restoring the E/I balance is a key strategy for epilepsy treatment [33–36]. Combining our current understanding with previous findings on GPR173 [29]., we demonstrated that CCK release activates GPR173, leading to Ca^{2+} signaling via postsynaptic channels or endoplasmic reticulum release, potentially facilitating GPR173-mediated iLTP. iLTP may also require calcium/calmodulin-dependent protein kinase II (CaMKII) activation, increased gephyrin levels, or recruitment of postsynaptic γ-Aminobutyric acid sub-type A receptors (GABAARs), as shown in other studies [37–40]. In contrast, targeting CCK3R offers a more precise modulation of inhibitory neurotransmission. This may potentially minimize the widespread side effects associated with GABA receptor-targeted drugs due to the extensive distribution of GABA receptors in the brain and their influence on numerous neural functions. Additionally, CCK3R activation may induce more robust and sustained iLTP, enhancing the overall inhibitory tone in neural circuits and improving seizure control. Moreover, CCK3R-targeted therapies could complement existing treatments by providing a novel mechanism of action, potentially addressing the unmet needs of patients resistant to current antiepileptic drugs [41]. Hence, CCK3R presents a promising alternative to GABA receptors for epilepsy treatment.

We hypothesized that CCK3R overexpression facilitates signaling that potentiates inhibition, thereby restoring the E/I balance in the brains of mice with chronic seizures. Animal models that mimic the behavioral, physiological, and anatomical deficits observed in human chronic epilepsy are crucial for developing new therapies and drug screening for epilepsy treatment. Notably, temporal lobe epilepsy, which represents the highest percentage of all acquired refractory epilepsy, is characterized by hippocampal lesions [42]. Thus, we established a chronic epilepsy model in mice by injecting kainic acid (KA) into the hippocampus according to our previous research [43]. Neuropeptides are preferentially released by neurons during high-frequency stimulation [44]. This preferential release makes CCK particularly attractive, as it is likely to be released during pathological hyperexcitability associated with seizures while having little effect on synaptic function during regular activity. In vitro patch-clamp recordings were performed to further verify that upregulation of GPR173 enhances iLTP in CCK-GABA synapses. Subsequently, we designed and delivered AAV vectors carrying the CCK3R gene to mice with chronic seizures to examine whether exogenous upregulation of the CCK3R could attenuate epilepsy. In addition, we conducted behavioral assays and in vitro patch-clamp recordings to evaluate the side effects of this gene therapy on typical behavioral manifestation, physiological functions, and functioning of brain neurons in mice. Our findings demonstrate that the recombinant AAV-GPR173 vector, driven by cytomegalovirus (CMV) and CaMKII promoters, mediates powerful anticonvulsant effects and substantially reduces seizure frequency. Behavioral assessments indicated increased active time and reduced anxiety-like behaviors without affecting recognition and learning ability in treated mice. These results suggest that the AAV-GPR173 vector may be safe in rodents and could be considered a vector of choice for potential clinical applications in epilepsy treatment.

RESULTS

Induction of a chronic epileptic mouse model via intrahippocampal KA injection

Our goal was to reduce seizures in a mouse model of chronic epilepsy. We effectively used intrahippocampal KA injection to create a mouse model of chronic epilepsy using C57BL/6 J male mice (Fig. 1A), a well-established chronic epilepsy model developed previously [45, 46]. This mouse model exhibits similarities in behavioral, physiological, and anatomical deficits with human chronic epilepsy [47]. In our study, we utilized this model and monitored the daily spontaneous seizures of the animals for 16 weeks using our mouse seizure recognition system (MMRS, Fig. 1B). Epileptic seizures were categorized into five stages based on a revised Racine scale: 1) mouth and facial movements, 2) head nodding, 3) forelimb clonus, 4) standing and rearing, and 5) jumping and falling [48]. However, for our 24-h behavioral observation and analysis, we included only stages 3–5 seizures during the following 16 weeks (Supplementary videos 1–3). Our results showed that recurrent convulsive seizures of stages 3–5 began in the second or third week after KA injection (Fig. 1C, Table S1). Once mice exhibited these seizures, they continued to experience them for the following 13 weeks (5.2 ± 1.52 per day at week 4). Some of the mice perished before the end of the 16-week observation period due to severe seizure attacks (as shown in Fig. 1D and E, in comparison to weeks 4 or 5; $N = 5$ mice; one-way analysis of variance [ANOVA] with Tukey's post hoc test, not significant [N.S.]). Moreover, the histological evaluation of glial fibrillary acidic protein^{+} (GFAP) cells (which serve as a marker for an abnormal increase in the number of astrocytes) in the right hippocampus (748.56 ± 74.88 per mm^2) after 16 weeks revealed that the right intrahippocampal KA injection caused reactivity of astrocytes (as depicted in Fig. 1F, which contains 10 sections from $N = 4$ mice). The emergence of spontaneous recurrent seizures and reactivity of astrocytes in the KA-injected hippocampus resembles human chronic epilepsy, suggesting that chronic seizures in mice can be employed in the study of chronic epilepsy treatment.

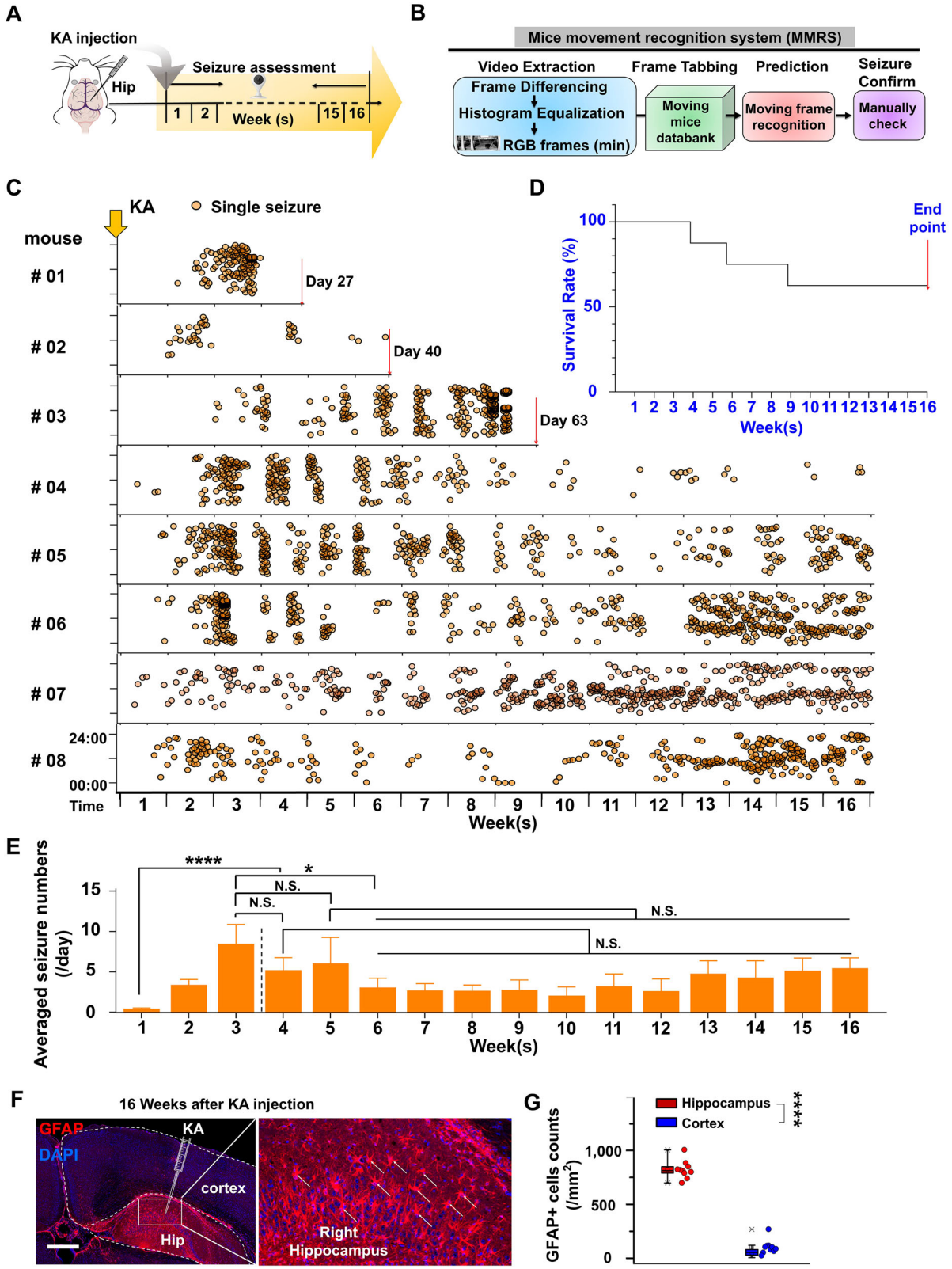

Fig. 1 Development of the epileptic mouse model via intrahippocampal kainic acid (KA) injection. A Schematic illustration of the intrahippocampal KA injection-induced epileptic mouse model. **B** Mice movement recognition system (MMRS). **C** Seizure occurrences in eight mice (after KA injection) without therapy. Each dot represents one seizure event. The y-axis represents the observation time over 24 h. **D** The survival rate of eight mice with chronic epilepsy. **E** Averaged daily seizures each week over 16 weeks (N = 5, one-way ANOVA with Tukey's post hoc test, $^{*}P < 0.05$; N.S.). **F** Immunohistochemistry images and group data for staining of glial fibrillary acidic protein in the chronic epileptic mice (scale bar: 500 μm; n = 10 sections, N = 4 mice; one-way ANOVA with Tukey's post hoc test, $^{****}P < 0.0001$). Data are expressed as mean ± standard error of the mean. ANOVA, analysis of variance; N.S.; not significant.

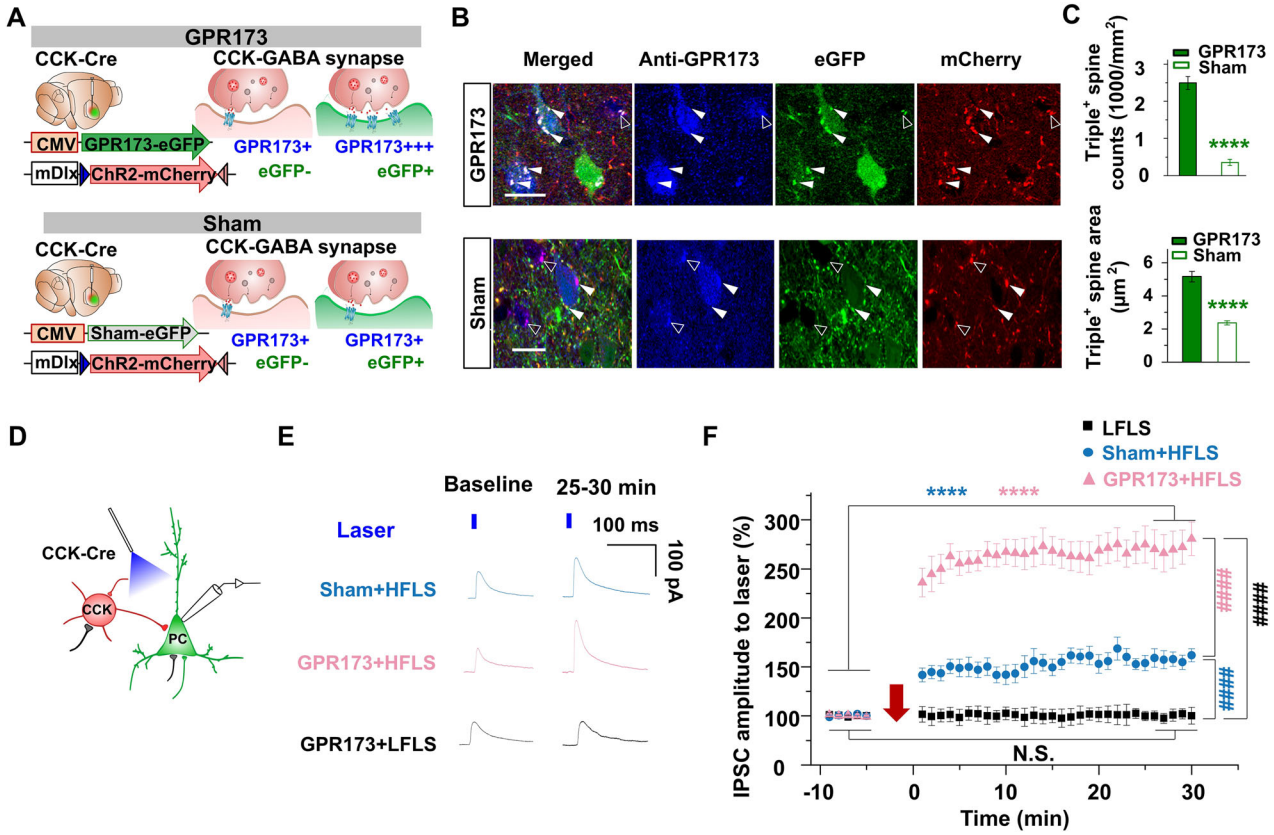

Fig. 2 Upregulation of GPR173 at the CCK-GABA synapses in the cortex enhances iLTP. A Schematic diagram showing the injection of mDlx-DIO-ChR2-mCherry and CMV GPR173-eGFP virus into the CCK-Cre (upper, GPR173), or the mDlx-DIO-ChR2-mCherry and CMV-Sham-eGFP virus into the CCK-Cre (lower, sham). **B** Confocal images of eGFP and mCherry reporter gene expression with GPR173 in the mDlx-DIO-ChR2-mCherry and CMV-GPR173-eGFP injected mice (upper panels) and mDlx-DIO-ChR2-mCherry and CMV-Sham-eGFP injected mice (lower panels; scale bars: 20 μm). **C Upper panel:** averaged counts of eGFP, mCherry, and GPR173 triple-labeling of the two groups per mm^2 in the region of interest (ROI) (GPR173: n = 9 sections, N = 4 mice; Sham: n = 9 sections, N = 4 mice; one-way ANOVA with Tukey's post hoc test, ****$P < 0.0001$); **Lower panel:** averaged area (μm^2) of eGFP, mCherry, and GPR173 triple-labeling of the two groups of ROI (mm^2) (GPR173: n = 9 sections, N = 4 mice; Sham: n = 9 sections, N = 4 mice; one-way ANOVA with Tukey's post hoc test, ****$P < 0.0001$). **D** Diagram for whole-cell patch-clamp recording in the cortical slice (PC: pyramidal cell). **E** Representative IPSC traces before (baseline) and 25–30 min after the HFLS of GABA-CCK neurons in the sham group (traces in blue), the HFLS of GABA-CCK neurons in the GPR173-injected group (traces in red), and the LFLS of GABA-CCK neurons in the GPR173-injected group (traces in black). **F** Time course of normalized IPSC before (for 5 min) and after (for 30 min) the HFLS at GPR173 group (red, n = 11 neurons), or the HFLS in the sham group (blue, n = 7 neurons), and the LFLS at GPR173 group (black, n = 11 neurons) (two-way RM ANOVA with Tukey's post hoc test, within-group comparison: ****$P < 0.0001$, N.S.; among groups comparison: ####$P < 0.0001$, N.S.; Data are expressed as the mean ± standard error of the mean). iLTP inhibitory long-term potentiation, IPSC inhibitory postsynaptic current, HFLS high-frequency laser stimulation; LFLS low-frequency laser stimulation, N.S. not significant, RM repeated measures, ANOVA analysis of variance, PC pyramidal cell.

Upregulation of GPR173 in the cortex induces enhanced iLTP by high-frequency laser stimulation (HFLS)

An imbalance in the E/I ratio in the brain can result in various brain disorders such as autism spectrum disorder, schizophrenia spectrum disorders [49, 50], and epilepsy [51]. Our previous study has shown that GPR173 mediates CCK signaling at the CCK-GABA synapse and potentiates its inhibition [29]. Therefore, we sought to restore the E/I balance in epilepsy by exogenously upregulating GPR173. We used a blood-brain barrier (BBB)-penetrating AAV to infect the entire brain rather than employing gene manipulation in limited brain regions. Neurons that express GPR173 include excitatory and inhibitory neurons. Approximately 90% of $GPR173^+$ cells were identified as $CaMKII^+$ neurons [29]. However, the specific role of GPR173 in these two neuronal types remains unclear. Further investigations are necessary to elucidate the specific functions of GPR173 in excitatory and inhibitory neurons. Consequently, we initially utilized the CMV promoter because it is a conventional promoter that provides high initial neural expression [52]. Our therapy involves the production of AAV-PHP.eB, carrying AAV-CMV-GPR173-eGFP-PHP.eB (hereafter referred to as CMV-GPR173-eGFP) or its sham control AAV-CMV-Sham-eGFP-PHP.eB (CMV-Sham-eGFP).

In the following experiment, we sought to determine whether CMV-GPR173-eGFP effectively increased GPR173 expression in the postsynaptic neuron of CCK-GABA terminals. To test this hypothesis, we injected a mixture of CMV-GPR173-eGFP and mDlx-DIO-ChR2-mCherry into the auditory cortex (ACx) of CCK-Cre mice (Fig. 2A, **upper panel**). Another group of CCK-Cre mice was administered a mixture of sham control CMV-Sham-eGFP and mDlx-DIO-ChR2-mCherry (Fig. 2A, **lower panel**). We conducted an anatomical verification of reporter eGFP, mCherry (CCK-GABA terminals and fibers), and GPR173 (endogenous and exogenous) expression. We showed the triple-labeling of eGFP, mCherry, and GPR173 (Table S2), indicating the potential presence of exogenously introduced GPR173 expression at 2 weeks after the virus injection (Fig. 2B). To confirm the expression of GPR173 at the desired site, we analyzed the number and size of eGFP, mCherry, and GPR173 triple-labeling. The results in Fig. 2C demonstrate that the CMV-GPR173-eGFP group expressed more GPR173 at postsynaptic neurons of CCK-GABA terminals than the sham control

CMV-Sham-eGFP group. The comparison was conducted by counting and analyzing the area of triple colocalization of the region of interest (ROI) between the GPR173 and sham groups. The results showed that the GPR173 group had significantly higher counts and area of triple colocalizations than the sham group (GPR173 vs. Sham: counts: 2496.89 ± 173.30 vs. 354.96 ± 83.36 per mm^2; area: 5.18 ± 0.32 vs. 2.37 ± 0.12 μm^2 per mm^2 of ROI; GPR173: n = 9 sections, N = 4 mice; Sham: n = 9 sections, N = 4 mice; one-way ANOVA with Tukey's post hoc test, ****$P < 0.0001$).

In our previous investigation [29], we conducted extracellular and in vitro patch-clamp recording experiments to examine the CCK-GPR173-dependent iLTP. Our findings demonstrated that iLTP was not induced in CCK-knockout (KO) mice but was observed in CCK1R/2 R double-KO mice. Furthermore, we utilized GPR173 antagonists and CCK-KO experiments in our previous study. These results indicate that GPR173, a novel CCK receptor, mediates CCK signaling from CCK interneurons and induces iLTP at post-synapses [29]. In the current study, we extended our previous in vitro patch-clamp recording experiments to investigate whether GPR173 upregulation could induce an amplified iLTP.

In the next step, we aimed to verify whether the upregulation of GPR173 enhances iLTP. To achieve this, we utilized brain slices from CCK-Cre mice for in vitro patch-clamp recording after 2 weeks of virus injection (Fig. 2A and D). Initially, we selectively patched pyramidal neurons in the virus-injected area of the AC, as previously described [29]. Next, we directly recorded the inhibitory post-synaptic current (IPSC) evoked by laser stimulation (0.15 Hz, 5 min as baseline) of GABA-CCK neurons transfected with mDlx-DIO-ChR2-mCherry (Fig. 2A). We observed a more pronounced potentiation of IPSC in the CMV-GPR173-eGFP-injected CCK-Cre mouse compared with the CMV-Sham-eGFP-injected CCK-Cre mouse after the HFLS of GABA-CCK neurons (Fig. 2D, single traces, and averaged traces of IPSC responses to the laser stimulation at 0.15 Hz, before and after the HFLS for 25–30 min; Fig. 2E, representative neuronal responses to the HFLS). The time course of normalized IPSC before (for 5 min) and after the HFLS (for 30 min) showed no significant potentiation of IPSC in the CMV-GPR173-eGFP-injected CCK-Cre mouse after the low-frequency laser stimulation (LFLS) (Fig. 2F, baseline vs. 25–30 min after LFLS: 100.17 ± 0.66% vs. 100.06 ± 1.66%, n = 13 neurons, two-way ANOVA with Tukey's post hoc test, N.S.), while the HFLS of CCK-GABA neurons induced a more significant IPSC potentiation in the CMV-GPR173-eGFP-injected CCK-Cre mice than in the CMV-Sham-eGFP-injected CCK-Cre mice (Fig. 2F, baseline vs. 25–30 min after HFLS at CMV-GPR173-eGFP-injected CCK-Cre mouse: 100.01 ± 1.54% vs. 271.69 ± 18.43%, n = 12 neurons, HFLS at CMV-Sham-eGFP-injected CCK-Cre mouse: 100.45 ± 1.45% vs. 158.15 ± 8.01%, n = 12 neurons, two-way ANOVA with Tukey's post hoc test, ****$P < 0.0001$).

Thus, the HFLS of GABA-CCK neurons in CMV-GPR173-eGFP-injected CCK-Cre mouse enhanced the potentiation of IPSC during the recording period, or iLTP, compared to the HFLS of GABA-CCK neurons in CMV-Sham-eGFP-injected CCK-Cre mouse (271.69 ± 18.43% vs. 158.15 ± 8.01%, two-way repeated measures (RM) ANOVA with Tukey's post hoc test, ####$P < 0.0001$). Furthermore, our results demonstrated that exogenously increasing GPR173 expression contributes to increased iLTP.

Long-term suppression of chronic seizures is observed after the overexpression of GPR173 via single-dose systemic administration of AAV promoted by CMV

The brains of individuals with epilepsy are characterized by recurrent episodes of heightened excitability in multiple brain regions during seizure attacks [2]. In this context, a practical and effective therapeutic approach is to increase the number of enhanced inhibitory synapses in epileptic mice, which can function as stopping points during the progression of hyperexcitability. In our previous study [29], we discovered that GPR173 facilitates iLTP in GABAergic CCK neurons. We propose that boosting the expression of GPR173 externally may enhance iLTP, restore the E/I balance in epileptic mice, and consequently suppress chronic seizures.

The findings shown in Fig. 2 suggest GPR173 as a promising target for treating epilepsy, given its role in regulating neuronal excitability in the cortex. To investigate its role, we increased the expression of GPR173 via the above CMV-GPR173-eGFP in epileptic mice to determine whether it could suppress chronic seizures. We injected KA into the CA1 region of the hippocampus to establish a chronic epileptic mouse model, as shown in (Fig. 3A). We recorded the number of seizures for 24 h manually, as shown in (Fig. 1). Additionally, we scored the seizure stages (Fig. 3B) according to the revised Racine scale [48]. Determining the optimal intervention time for AAV is crucial, considering its effectiveness and efficiency in suppressing seizures. According to video monitoring, the mouse typically demonstrated a combination of stages 3, 4, and 5 seizures within one seizure attack (Supplementary videos 4–6). No reduction in the frequency of these behaviors were observed during the 13 weeks after KA injection (Fig. 1C–E). As week 3 demonstrated an unstable seizure frequency (Fig. 1), it was not included in the pretreatment levels. We recorded the seizures of each mouse for 13 weeks, including week 4 and 5 after KA injection, as the baseline before treatment (Fig. 3C, **before**). Subsequently, we administered CMV-GPR173-eGFP (50 µL, 5.01 E + 12 viral genomes per milliliter (vg/mL), experimental group) or CMV-Sham-eGFP (50 µL, 5.32 E + 12 vg/mL, control group) to the transverse venous sinus of each mouse (Fig. 3A). We then observed seizures in the subsequent 8 weeks (Fig. 3C and D, **after**). We assigned scores ranging from 1 to 3 for seizures occurring in stages 3 to 5, respectively. During this scoring process, most seizures were classified as Stage 5. Notably, when the mice exhibited a stage 4 seizure, it was invariably followed by a stage 5 seizure (Fig. 3B). Given the limited availability of mice with chronic epilepsy, we opted for intravenous administration to maximize the probability of successful viral delivery. To ensure adequate viral delivery, the solution was injected under a microscope.

Our observations revealed a significant decrease in seizures in mice administered CMV-GPR173-eGFP during the initial 2-week period after intervention (Fig. 3D; weeks 6–7 vs. baseline weeks 4–5: 0.74 ± 0.23 vs. 2.08 ± 0.54, ***$P < 0.001$, N = 8), and this trend continued for the subsequent 2-week period (Fig. 3E; weeks 8–9 vs. baseline weeks 4–5: 0.47 ± 0.12 vs. 2.08 ± 0.54, ****$P < 0.0001$). Notably, the mice in the experimental group maintained low seizure levels throughout the observation period, extending up to week 13 (Fig. 3E; weeks 10–11 vs. baseline weeks 4–5: 0.30 ± 0.07 vs. 2.08 ± 0.54, $P < 0.0001$; weeks 12–13, 0.45 ± 0.11 vs. 2.08 ± 0.54, ****$P < 0.0001$). In contrast, the control group mice (CMV-Sham-eGFP) showed no change in seizure frequency during the initial and second 2-week periods after treatment (Fig. 3D, weeks 6–7 vs. baseline weeks 4–5:2.23 ± 0.54 vs. 2.68 ± 1.07, $P = 0.726$, weeks 8–9 vs. baseline weeks 4–5: 3.40 ± 1.14 vs. 2.68 ± 1.07, $P = 0.650$, N = 8) but exhibited a significant increase in seizures starting from week 10 (Fig. 3D, weeks 10–11 vs. baseline: 6.17 ± 1.50 vs. 2.68 ± 1.07, $P = 0.107$, weeks 12–13 vs. baseline: 6.08 ± 1.39 vs. 2.68 ± 1.07, $P = 0.096$, N = 8). These results suggest that CMV-GPR173-eGFP effectively modulates inhibitory control and reduces the overall network hyperexcitability in the epileptic brain, thereby decreasing the likelihood of seizure initiation.

When utilizing AAV vectors for treating neurological disorders, ensuring transgene expression in target cells, AAV vector passage across the BBB, and sustained long-term expression in the desired brain region after a single injection are critical considerations. To investigate these factors, we conducted anatomical analyses of the brain from the CMV-GPR173-eGFP and CMV-Sham-eGFP-injected groups 6 months after virus injection. Consistent

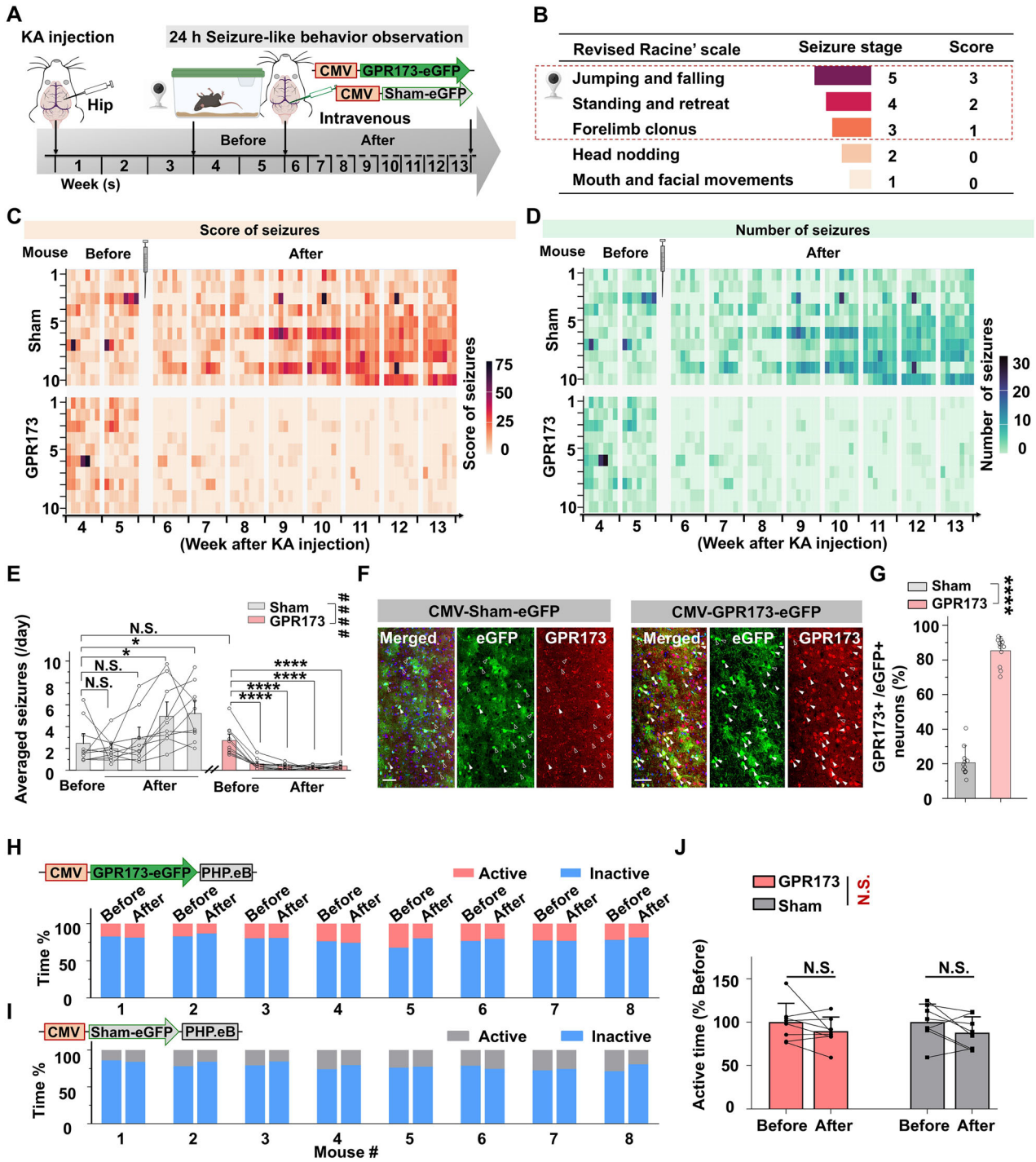

detection of eGFP in the neocortex confirmed that intravenous infusion of AAV/PHP.eB successfully penetrated the BBB. We also co-labeled GPR173 with eGFP to confirm AAV specificity (Fig. 3F). We quantified the percentage of GPR173$^+$ cells among the eGFP$^+$ cells. In the CMV-GPR173-eGFP-injected group, 89% of eGFP$^+$ cells expressed GPR173, whereas only 20% of eGFP$^+$ cells showed GPR173 positivity in the sham group (Fig. 3G). Our findings demonstrated that the CMV-GPR173-eGFP-injected mouse introduced more exogenous GPR173 after a single dose of AAV injection than the CMV-Sham-eGFP-injected mice.

We initially explored the possibility of adverse effects on behavior and structure resulting from gene therapy. By comparing the activity time from our video data after virus injection in both groups, we found no significant difference in the amount of activity time between the CMV-GPR173-eGFP and sham control CMV-Sham-eGFP groups (Fig. 3H–J; one-way ANOVA with Tukey's post hoc test, N.S.). In conclusion, our observations over 8 weeks suggest that a single dose of exogenous GPR173 delivered through gene therapy was effective in successfully suppressing chronic seizures in mice in the long term.

C-fos expression reveals cortical excitatory neuronal hyperactivity after KA-induced chronic seizures

Based on our previous research [43], it has been discovered that the network pathology observed in chronic epilepsy is not limited to the hippocampus; rather, remote non-hippocampal structures

Fig. 3 Upregulation of GPR173-containing AAV vector suppressed kainic acid (KA)-induced epilepsy in mice via CMV-GPR173-eGFP. **A** Schematic illustration of the gene therapy timeline used to inhibit intra-hippocampal KA injection-induced epilepsy. After 3 weeks of intrahippocampal KA injection, 2 weeks of seizure observation were performed (**Before**). After intravenous viral (rAAV-CMV-GPR173-eGFP or rAAV-CMV-eGFP) delivery, the mice were continuously monitored for seizures for 8 weeks (**After**). **B** Mice seizure recognition system (MSRS). **C** Heat maps of the score of seizures detected daily in the CMV-Sham-eGFP injected mice (upper panel, N = 10) and CMV-GPR173-eGFP injected mice (lower panel, N = 10). **D** Heat maps of the number of seizures detected daily in the CMV-Sham-eGFP injected mice (upper panel, N = 10) and CMV-GPR173-eGFP injected mice (lower panel, N = 10). **E** Bar chart for the average number of seizures per mouse within 2 weeks **Before** and **After** therapy (per 2 weeks, total 8 weeks; CMV-Sham-eGFP group in grey, N = 8; CMV-GPR173-eGFP group in red, N = 8; one-way ANOVA with Tukey's post hoc test, $^{*}P < 0.05$, $^{****}P < 0.0001$; N.S.; two-way RM ANOVA with Tukey's post hoc test, $^{\#\#\#\#}P < 0.0001$, N.S.). **F** Confocal images of eGFP reporter gene expression with GPR173 in the cortex of CMV-Sham-eGFP injected mice (left panels) or CMV-GPR173-eGFP injected mice (right panels; scale bars: 5 μm). **G** Percentage of eGFP and GPR173 co-labeling in the two groups (GPR173: n = 12 sections, N = 5 mice; Sham: n = 9 sections, N = 3 mice; one-way ANOVA with Tukey's post hoc test, $^{****}P < 0.0001$). **H** Percentage stacked bar charts for the average active (pink) and inactive time (blue) of each chronic epilepsy mouse, intravenously injected with CMV-GPR173-eGFP. **I** Percentage stacked bar charts for the average active time (grey) and inactive time (blue) of each chronic epilepsy mouse intravenously injected with CMV-Sham-eGFP. **J** Group data showing the comparison of active time within and between the two groups (GPR173, N = 8; Sham, N = 8; one-way ANOVA with Tukey's post hoc test, N.S.). Data are expressed as mean ± standard error of the mean. AAV adeno-associated virus, N.S. not significant, RM repeated measures, ANOVA analysis of variance.

such as the motor cortex (MCx), visual cortex (VCx), and ACx are involved. Following spontaneous seizures in KA-induced chronic epilepsy, prominent labeling of c-fos^{+} cells was observed in both the hippocampus and non-hippocampal structures [43].

As demonstrated in Fig. 3, the exogenous upregulation of GPR173, promoted by the CMV promoter, suppressed chronic seizures. Using CMV-GPR173, we labeled the excitatory neurons, inhibitory neurons, and astrocytes (Fig. 3F). We hypothesized that GPR173 expressed in cortical excitatory neurons predominantly mediates the antiepileptic effects. Before specifying the expression of GPR173 in excitatory neurons promoted by the CaMKII promoter, we lacked evidence that cortical excitatory neurons are excessively active during chronic seizures. Consequently, we co-labeled CaMKII and c-fos in the cortex (including the MCx, VCx, and ACx) to demonstrate that excitatory neurons exhibited excessive activity during chronic seizures. According to previous observations (Figs. 1A and 3A), chronic spontaneous seizures have been developed and maintained for at least 13 weeks. Thus, we continuously monitored seizures for 10 weeks in the home cage, as shown in Fig. 4A and B. After confirming the successful establishment of stable seizures, three mice per group were observed in real-time within a recording chamber. Owing to the constraints of manual observation, three epileptic mice were continuously monitored simultaneously until seizures were observed. Subsequently, 90 min after the occurrence of spontaneous seizures, the epileptic mice were perfused. This process was repeated until five epileptic mice were obtained. As a control, saline-injected age-matched mice, which did not experience seizures, were perfused. All brains were carefully extracted and processed for immunohistochemical analysis. We then performed co-staining for CaMKII and c-fos (an immediate early gene, a marker of neuronal activation) to identify regions of increased activity during seizures, on slices from the epileptic mice and non-seizure saline group, which served as the baseline for c-fos expression. Our results showed that a substantial number of cortical excitatory neurons expressed c-fos in slices from KA-induced epileptic mice, as shown in Fig. 4C and D (KA-injected mice after spontaneous seizures vs. saline-injected mice without spontaneous seizures, in MCx: 110.95 ± 6.99 vs. 8.46 ± 1.88, VCx: 96.92 ± 6.55 vs. 20.62 ± 2.22, and ACx: 100.18 ± 9.12 vs. 20.29 ± 2.57 merged cells/mm^2, $^{****}P < 0.0001$; n = 16–18 slices, N = 5 mice for each group). Quantification of c-fos-positive excitatory neurons revealed significant differences in the cortex associated with seizure activity between the epileptic and control mice. This finding suggests that cortical excitatory neurons were widely recruited during spontaneous seizures.

The propensity for heightened activity and synchronized firing among a considerable number of cortical excitatory neurons in epileptic mice implies that targeting GPR173 delivery to these excitatory neurons globally may offer a promising approach to curing chronic epilepsy.

Upregulation of GPR173 in excitatory cortical neurons results in a reduction of seizures in mice through single-dose systemic administration of AAV-CaMKII-GPR173

In epilepsy research, it has been demonstrated that the optogenetic inhibition of excitatory neurons or activation of inhibitory interneurons effectively reduces seizure activity in preclinical models [53, 54]. Despite the potential of existing approaches, their clinical translation has been hindered by the need for invasive surgical procedures to implant optical hardware and the potential for off-target effects of broad neuronal manipulation. To overcome these challenges, we plan to develop a novel gene therapy that targets cortical excitatory neurons by systematically upregulating GPR173, which plays a critical role in regulating network excitability via enhanced inhibition (Fig. 2) [29]. Following a series of kindled seizures, research has shown that CCK mRNA expression is elevated in certain GABAergic neurons in the amygdala, cerebral cortex, and hippocampus [55, 56]. This may be attributed to the fact that GABAergic neurons are more readily activated during seizures, which can lead to the release of neuronal peptides, including CCK. To enhance the GABAergic inhibitory effect and rapidly terminate seizures precisely, we aimed to selectively express more CCK3R (GPR173) in excitatory neurons. Although we successfully administered the virus intravenously and observed its impact on chronic epileptic mouse models (Fig. 3), the entire procedure is notably time intensive and requires substantial effort. Craniotomy poses risks to mouse health and is associated with relatively low success rates. In our preparations to substitute the viral promoter with CaMKII, we identified an auxiliary tool that facilitates tail vein injection, enabling more efficient and precise experimental execution. Consequently, we used tail vein injections in the following treatments.

To explore the potential therapeutic benefits of GPR173 upregulation in cortical excitatory neurons, we used a well-established mouse model of KA-induced chronic epilepsy, as previously described (Figs. 1 and 3). Following the development of the epileptic mouse model, the mice were monitored for spontaneous seizures for 5 weeks to maintain consistency across the experiments (Figs. 1 and 3). At weeks 4 and 5, subsequently defined as the baseline, the mice were randomly divided into three groups for AAV vector administration (Supplementary videos 7–9). These groups received the same volume of saline, AAV-CaMKII-GPR173-mCherry, or control vector AAV-CaMKII-Sham-mCherry via tail vein injection (Fig. 5A). The mice were then continuously monitored for seizure activity using video recordings for an additional 8 weeks (weeks 6–13). Compared with the two control groups, mice that overexpressed GPR173

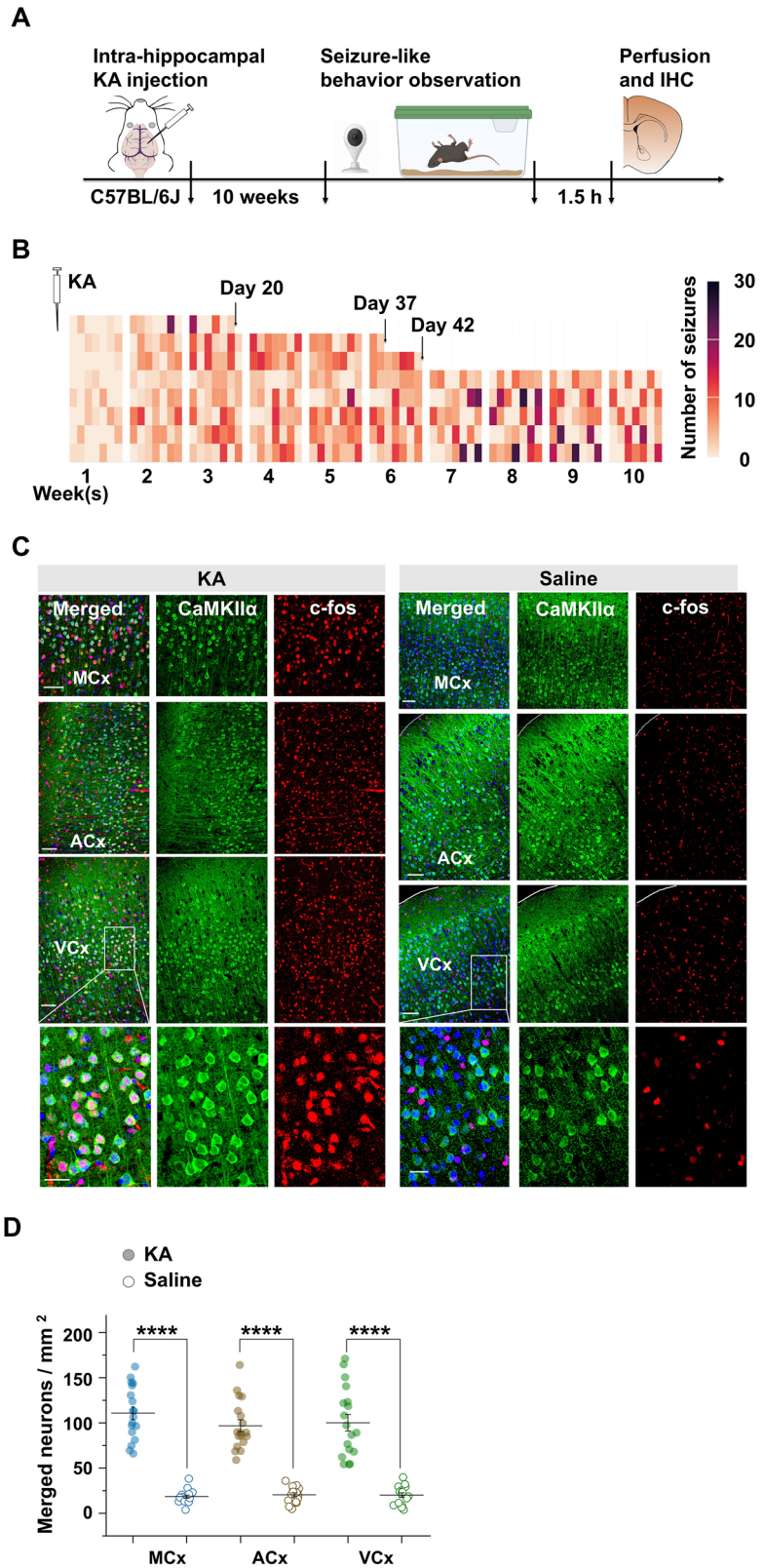

Fig. 4 C-fos expression reveals cortical excitatory neuronal hyperactivity after kainic acid (KA)-induced chronic seizures. A Schematic illustration of the experimental timeline used to develop a mouse model of chronic seizure. **B** Heat maps of the number of seizures detected daily in KA-injected mice (N = 8). **C** Confocal images of co-labeling of CaMKII and c-fos from MCx, ACx, and VCx of mice injected with KA and saline (scale bars: 100 μm, 50 μm). **D** Group data showing the co-labeling of CaMKII and c-fos in the two groups (mice injected with KA, N = 5; mice injected with saline, N = 5; one-way ANOVA with Tukey's post hoc test, $^{****}P < 0.0001$). MCx Motor Cortex, ACx Auditory Cortex, VCx Visual Cortex, ANOVA analysis of variance.

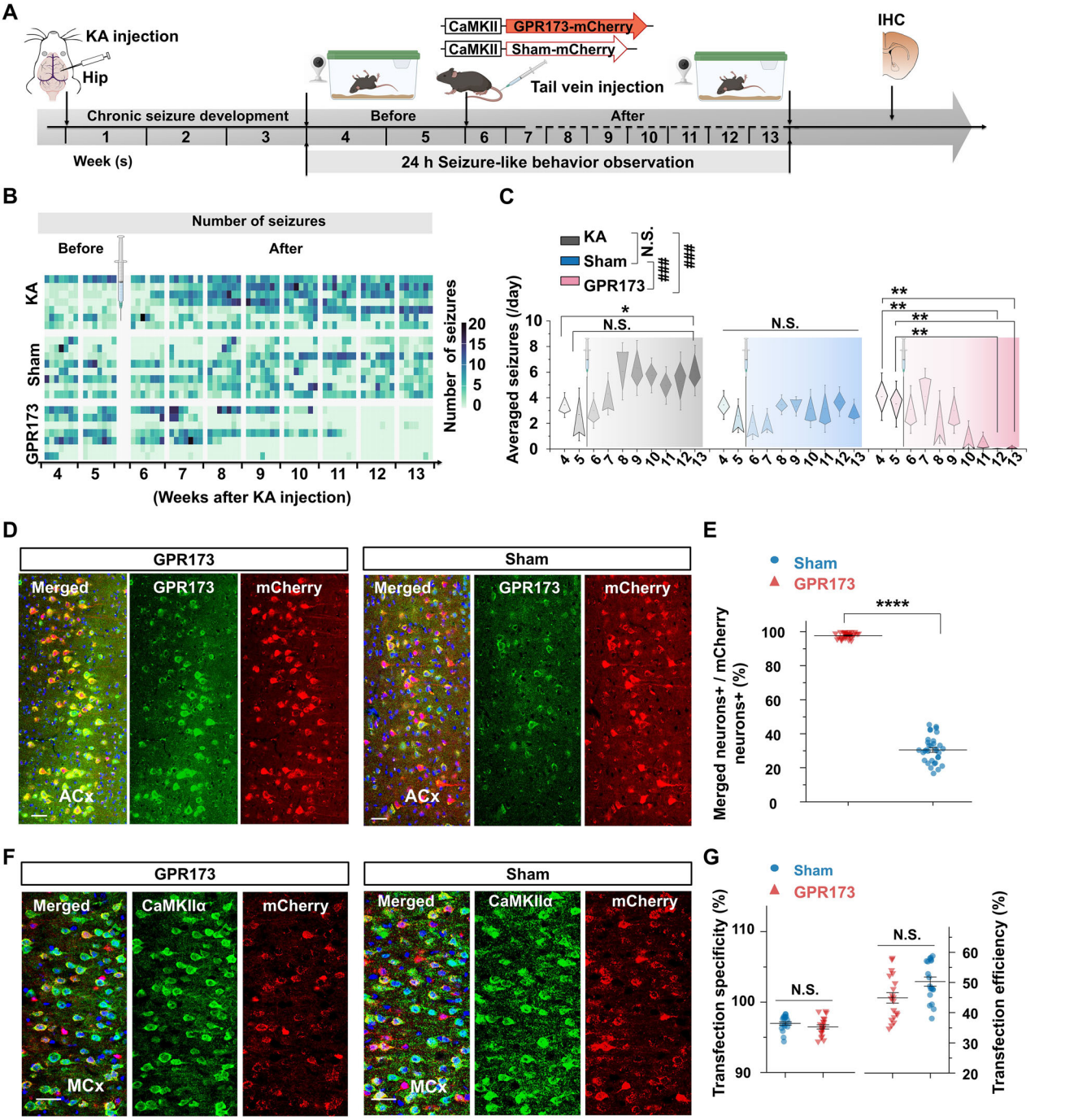

Fig. 5 Overexpression of GPR173 in excitatory neurons suppressed kainic acid (KA)-induced seizures in mice via the synthetic virus CaMKII-GPR173-mCherry. A Experimental diagram showing the surgery timeline, intrahippocampal KA injection, epilepsy observation, AAV injection, and histology. After 3 weeks of intrahippocampal KA injection, 2 weeks of seizure observation were performed (**Before**). After intravenous viral (rAAV-CaMKII-GPR173-mCherry or rAAV-CaMKII-Sham-mCherry) delivery, the animals were continuously monitored for seizures for 8 weeks (**After**). **B** Heat maps of the number of seizures detected daily in the KA-injected mice (upper panel, N = 7), CaMKII-Sham-mCherry injected mice (middle panel, N = 8), and CaMKII-GPR173-mCherry injected mice (lower panel, N = 7). **C** Box chart for the average number of seizures per mouse within 2 weeks **Before** and **After** therapy (per week, total 8 weeks; KA group, N = 7, $^{*}P < 0.05$; CaMKII-Sham-mCherry group, N = 8; CaMKII-GPR173-mCherry group, N = 7; one-way ANOVA with Tukey's post hoc test, $^{**}P < 0.01$; N.S.; one-way ANOVA with Tukey's post hoc test, $^{\#\#\#}P < 0.001$; N.S.). **D** Confirmation of mCherry reporter gene expression in the intravenously viral-injected chronic epileptic mice after the observation of seizures (left panel: CaMKII-GPR173-mCherry group; right panel: CaMKII-Sham-mCherry group; scale bars: 50 μm, respectively). **E** Percentage of mCherry and GPR173 co-labeling in the two groups (CaMKII-GPR173-mCherry group: N = 3 mice; CaMKII-Sham-mCherry group: N = 3 mice). **F** Confocal images of mCherry reporter gene expression with CaMKII in the cortex of CaMKII-GPR173-mCherry (left panels) or CaMKII-Sham-mCherry injected mice (right panels; scale bars: 50 μm). **G** Group data of CaMKII and mCherry co-labeling in the two groups. The transfection specificity means the proportion of CaMKII immunopositivity in the mCherry-expressing neurons, the transfection efficiency represents the proportion of CaMKII neurons transfected by the AAV (CaMKII-GPR173-mCherry group: N = 3 mice; CaMKII-Sham-mCherry group: N = 3 mice; one-way ANOVA with Tukey's post hoc test, N.S.). Data are expressed as mean ± standard error of the mean. AAV adeno-associated virus, N.S. not significant, ANOVA analysis of variance.

exhibited a significant reduction in seizure frequency, particularly during the last 2 weeks of monitoring (Fig. 5B and C, GPR173-injected mice: week 12 vs. week 4: 0.02 ± 0.02 vs. 4.08 ± 1.24, $^{**}P = 0.0013$; week 13 vs. week 4: 0.14 ± 0.09 vs. 4.08 ± 1.24, $^{**}P = 0.0014$). Meanwhile, saline-injected mice increased seizure frequency from 2.31 ± 0.83 (week 4) to 6.12 ± 1.22 (week 13, $^{*}P = 0.034$). Notably, 4 mice from the GPR173-injected group did not experience seizures during the last 20 days. The total number of seizures in the first week before AAV administration was 172 in seven mice, which decreased to one in week 7 and seven seizures at week 8. Our observations revealed a notable reduction in the average number of spontaneous seizures at week 13 in the mice administered with AAV-CaMKII-GPR173-mCherry (at week 13, GPR173 vs. Sham vs. Saline: 0.14 ± 0.09 vs. 2.95 ± 0.62 vs. 6.12 ± 1.22, $\#\#\#P = 0.0007$ and 0.0001, respectively). Contrarily, neither the frequency nor the total number of seizures decreased in the saline and sham control groups (Fig. 5B and C, sham-injected mice: week 13 vs. week 5: 2.94 ± 0.62 vs. 2.59 ± 0.88, $P = 0.745$; saline-injected mice: week 13 vs. week 5: 6.12 ± 1.22 vs. 2.69 ± 1.27, $P = 0.097$).

To assess the potency and specificity of AAV, we first evaluated transgene expression 6 months after AAV injection. Immunohistochemistry demonstrated high transduction and sustained mCherry expression in GPR173 and sham groups. Histological analyses of co-labeling between GPR173 and mCherry revealed that GPR173 was upregulated in the ACx of mice that received AAV-CaMKII-GPR173-mCherry compared to those that received AAV-CaMKII-Sham-mCherry (Fig. 5D and E; 97.77 ± 0.27% vs. 30.49 ± 1.35%). Further examination using markers of excitatory neurons, CaMKII, showed that AAV carried the GPR173 gene into the appropriate neurons. Group data indicated that 96.98 ± 0.25% of mCherry^{+} neurons were also CaMKII^{+}, indicating that AAV possesses good specificity with no off-target effects. Furthermore, 50.30 ± 1.52% transfection efficiency suggests that we can effectively recruit a substantial number of targeted neurons with a single dose of AAV (Fig. 5F and G). We found a noticeable reduction in seizures of several mice starting from week 7 (Figs. 3 and 5B). Thus, we also examined the expression of GPR173 after 10 days (week 7) after viral delivery (Supplementary Figs. 1A and B). GPR173 was upregulated in the MCx and ACx of mice that received AAV-CaMKII-GPR173-mCherry (Supplementary Fig. 1C, AAV-CaMKII-GPR173 vs. AAV-CaMKII-Sham: 60.25 ± 1.52% vs. 31.87 ± 0.71%). Due to the limitation of histology and competitive expression of mCherry and GPR173 in neurons within 10 days, we labeled 60.25 ± 1.52% of mCherry^{+} neurons expressing GPR173 (Supplementary Fig. 1C). Given that CMV is a more robust promoter than CaMKII, enhancing gene expression in the brain, it is plausible to speculate that CMV-GPR173 could be expressed earlier than ten days, potentially explaining the immediate antiepileptic effect of CMV-GPR173 observed in some mice. These experimental findings highlight the effectiveness of AAV as a vector for gene delivery and expression, specifically targeting the GPR173 gene in excitatory neurons within the ACx. The observed high transduction efficiency and persistent expression over 6 months provide evidence of the long-term stability of the viral vector. Moreover, the substantial increase in GPR173 expression observed in the AAV-CaMKII-GPR173-mCherry group compared to the control cohort indicates successful upregulation of the target gene.

We observed that GPR173 expression was promoted by the CMV promoter. Subsequently, after observing a notable anti-epileptic effect of GPR173 upregulation (Fig. 3), we applied the specific promoter CaMKII to assess whether we could achieve the same therapeutic effect. This approach allowed us to establish the overall efficacy of GPR173 overexpression in epilepsy before targeting specific neuronal populations. Using the CaMKII promoter in subsequent experiments enabled us to focus on excitatory neurons (Fig. 5), which constitute the majority of the GPR173-expressing cells. By comparing the results from both promoters, we gained insights into the cell type-specific contributions of GPR173 to epilepsy suppression. These findings, obtained in a rodent model of KA-induced chronic epilepsy, suggest that targeting the GPR173 or its signaling pathway could be a novel and effective therapeutic approach for managing chronic epilepsy.

Long-term AAV-mediated GPR173 upregulation did not induce impairment of physiological functions or memory loss

Gene therapy offers the potential for long-term improvement of various monogenic genetic disorders with only one treatment. The success of such treatments depends not only on the extent of the therapeutic effect but also on the duration, which is contingent upon the sustained expression of the transgene. However, given the known adverse effects of anti-epileptic medications (e.g., fatigue, light-headedness, drowsiness, headaches, anxiety, depression, involuntary muscle contractions, and unsteady limbs) [57–59], we conducted behavioral tests to evaluate potential long-term side effects of gene therapy. To assess the impact of GPR173 upregulation on behavior, we administered a comprehensive battery of cognitive and behavioral tests to normal mice, as it would be challenging to examine the side effects directly on epileptic mice due to the significant epileptic effects on the brain.

Here, we aimed to investigate the behavioral changes induced by gene therapy in mice through the upregulation of GPR173 levels, which could potentially predict the impairment of physiological functions. To assess this, we used three tests: open field test (OFT), novel object recognition test (NORT), and Morris water maze test (MWMT) (Fig. 6A). Table S3 shows that two distinct cohorts of mice were employed for separate experimental purposes: one cohort was used to evaluate the therapeutic potential of GPR173-mediated gene therapy (Fig. 5), while the other was used to assess potential effects associated with viral vector administration (Fig. 6). Before and 12 weeks after AAV administration, we conducted the OFT across three groups to examine whether the upregulation of GPR173 caused anxiety-related behaviors. Our results (Fig. 6B and C**)** revealed that the proportion of time mice spent in the central area of the open field was comparable among the saline-, sham-, and GPR173-injected groups. Furthermore, we observed that the mice receiving GPR173 maintained similar activity levels after 12 weeks of AAV expression, while the other two groups exhibited a slight decrease in activity levels attributable to the natural aging process (Fig. 6D**;** Before vs. After, saline: 4067.53 ± 192.07 vs. 3046.80 ± 204.17; sham: 4549.74 ± 286.32 vs. 3016.81 ± 163.05; GPR173: 4136.49 ± 165.22 vs. 4447.90 ± 270.17; within-group comparison: $^{**}P < 0.01$, $^{***}P < 0.001$; among group comparison: $\#\#\#P < 0.001$). The results indicate that the upregulation of GPR173 does not elicit anxiety-related behaviors in mice, as evidenced by the comparable duration spent in the central area across all experimental groups. Notably, the GPR173-injected mice maintained consistent activity levels throughout the 12-week study period, whereas the saline and sham groups exhibited a decline in activity. Given that the duration spent in the center was comparable across groups, the total distance covered by the GPR173-injected group remained significantly greater than that of the saline- or sham-injected groups 12 weeks after injection. The findings suggest that GPR173 upregulation may not lead to significant cognitive side effects while counteracting age-related declines in locomotor activity. Further research is needed to understand the mechanisms through which GPR173 supports locomotor activity in older mice. Additionally, long-term studies assessing the effects of GPR173 upregulation on other cognitive and physiological aspects could provide valuable insights into its potential as a target for interventions aimed at promoting healthy aging.

We next aimed to investigate whether the upregulation of GPR173 leads to memory loss following the long-term expression

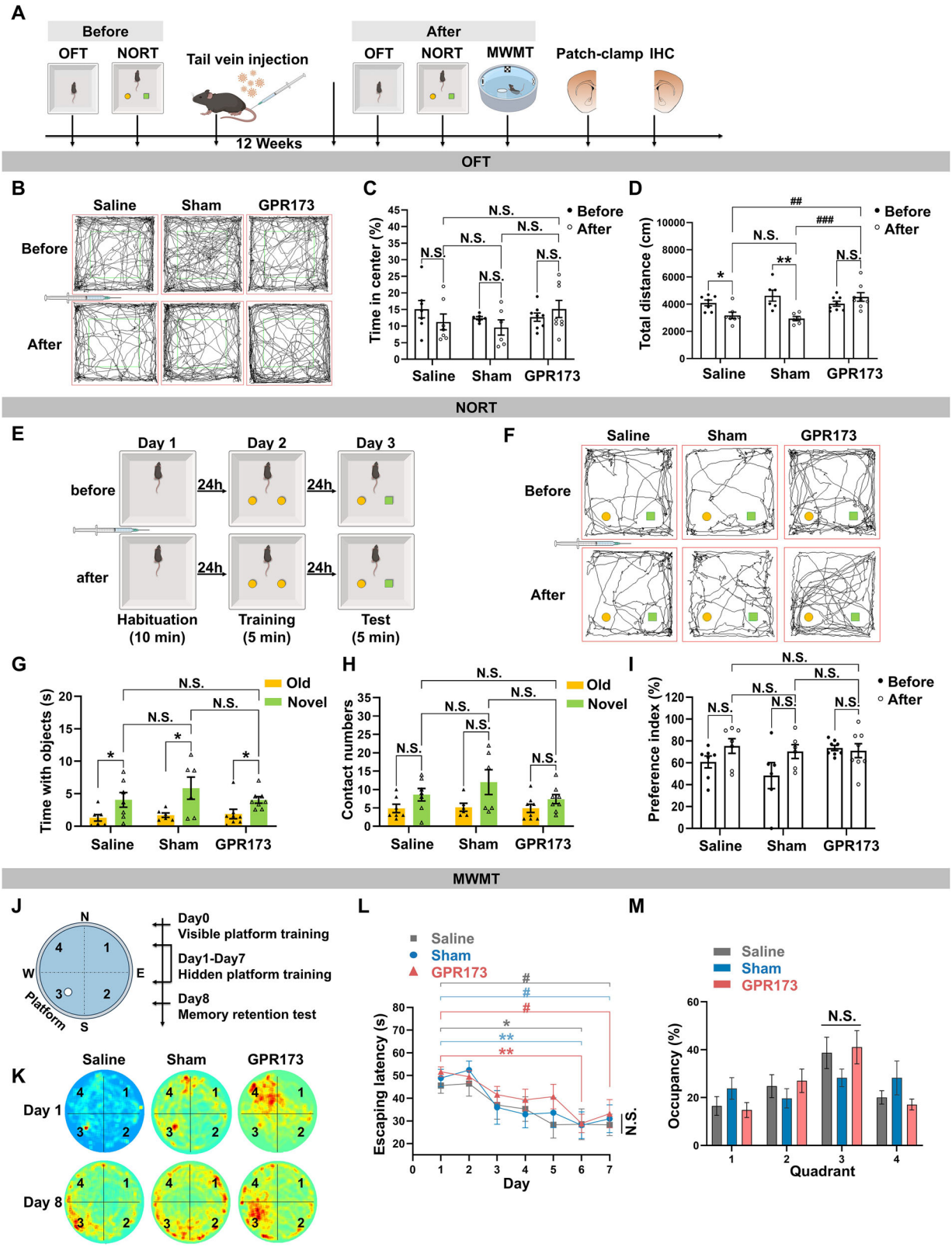

of AAV utilizing NORT and MWMT. As depicted in Fig. 6E and F, mice were habituated for 10 min on the first day, trained for 5 min on the second day, and tested on the third day. We recorded the number of contacts and the time spent with the old and new objects for each mouse. The results shown in Fig. 6G and H indicate that mice from the saline, sham, and GPR173 groups all preferred interacting with novel objects. The preference index in Fig. 6I demonstrates that AAV administration did not have an impact on memory performance, as there were no significant differences between the before and after test results for any of the

Fig. 6 Long-term AAV-mediated GPR173 upregulation does not induce any anxiety-like behavior or memory loss. A Schematic illustration of the timeline of the open field test (OFT), novel object recognition test (NORT), single dose AAV injection via tail vein, Morris water maze test (MWMT), whole-cell patch-clamp, and immunochemistry. After 12 weeks of virus expression, OFT and NORT were performed again, followed by MWMT (**After**). At last, mice were perfused for patch-clamp and immunohistochemical assays. All indicators were compared before and after tail vein injection in OFT and NORT. **B** Examples of trajectory diagrams of mice treated with saline, CaMKII-Sham-mCherry, or CaMKII-GPR173-mCherry in OFT, while the red frame represents the entire open field area, and the green frame represents the central area. **C** Group data showing the comparison of time spent in the center within and among the 3 groups (two-tailed two-sample t-test, N.S.). **D** Total distance traveled from the three groups of mice in the open field area (two-tailed two-sample t-test, within-group comparison: $^{**}P < 0.01$, $^{***}P < 0.001$; among groups comparison: $\#\#\#P < 0.001$; N.S.). In OFT, saline group, N = 9; CaMKII-Sham-mCherry group, N = 10; CaMKII-GPR173-mCherry group, N = 10. **E** Schematic illustration of the NORT protocol. **F** Examples of trajectory diagrams of mice in NORT, where the red frame indicates the entire movement area and the yellow and green objects inside indicate the old and novel objects, respectively. **G** Comparison of the time mice spent in contact with each object after viral injection (two-tailed two-sample t-test, within-group comparison: $^{*}P < 0.05$; among groups comparison: $\#P < 0.05$; N.S.). **H** The number of contacts between the mouse and each object after viral injection (two-tailed two-sample t-test, N.S.). **I** Preference index of mice for objects before and after tail vein injection (two-tailed two-sample t-test, N.S.). In NORT, saline group, N = 7; CaMKII-Sham-mCherry group, N = 6; CaMKII-GPR173-mCherry group, N = 8. **J** Diagram illustrating MWMT. Four quadrants are indicated as 1–4. Platforms are represented by the circle in quadrant 3. **K** Heat map of the movement trajectory of mice on day 1 and day 8. **L** Escape latency for the mice reaching the platform during training days 1–7 (two-tailed two-sample t-test, day 1 vs. day 6: $^{*}P < 0.05$, $^{**}P < 0.01$; day 1 vs. day 7: $\#P < 0.05$; one-way ANOVA with Tukey's post hoc test, N.S.). **M** The proportion of time mice spent in each quadrant during the day 8 test session (one-way ANOVA with Tukey's post hoc test, N.S.). In MWMT, saline group, N = 10; CaMKII-Sham-mCherry group, N = 9; CaMKII-GPR173-mCherry group, N = 9. Data are shown as mean ± standard error of the mean. AAV adeno-associated virus, N.S. not significant ANOVA analysis of variance.

groups (numbers of recruited animals showed in Table S4): saline (60.83 ± 5.50 vs. 75.39 ± 6.74), sham (56.89 ± 6.74 vs. 70.28 ± 6.31), or GPR173 (71.57 ± 2.38 vs. 71.12 ± 6.42).

Additional examinations were conducted using MWMT to assess spatial memory. We conducted the MWMT following Vorhees' protocol [60]. As depicted in Fig. 6J, the mice were trained for 7 days before testing. The time spent by mice reaching the platform during the training period was recorded. Compared to day 1, the GPR173, sham, and saline-injected groups all exhibited improved performance on day 6 (Fig. 6L, day 1 vs. day 6: Saline: 44.09 ± 2.54 vs. 29.43 ± 5.41; Sham: 47.62 ± 5.01 vs. 26.22 ± 4.52; GPR173: 52.59 ± 2.16 vs. 32.36 ± 4.98; day 1 vs. day 6: $^{*}P < 0.05$, $^{**}P < 0.01$; day 1 vs. day 7: $\#P < 0.05$). During the day 8 test session, the proportion of time the mice spent in each quadrant was evaluated (Fig. 6M), revealing that they remembered the location of the platform in the third quadrant, where it was placed during training.

Thus, our results indicate that the upregulation of GPR173 expression may not adversely affect normal behavioral outcomes or induce toxicity. Consequently, our findings suggest that the upregulation of GPR173 expression may constitute a viable therapeutic approach for treating chronic epilepsy. Clinical trials investigating GPR173-targeted therapies should meticulously monitor for potential adverse effects, although our data suggests a favorable safety profile.

AAV drives long-term expression of GPR173 without provoking abnormal firing characteristics in transfected excitatory neurons

One of the defining characteristics of chronic epilepsy is the imbalance between excitatory and inhibitory neurotransmitter systems in the brain [61]. In epilepsy, excitatory neurotransmission mediated by glutamate often increases, whereas inhibitory neurotransmission mediated by GABAergic decreases. This shift in the E/I balance can lead to the generation of abnormal neuronal firing patterns and seizures [62]. Subsequently, we aimed to ascertain whether GPR173 could regulate the excitability of cortical excitatory neurons. To achieve this, we analyzed the excitability of mCherry-tagged GPR173-expressing neurons using whole-cell patch-clamp recordings.

To assess whether sustained expression of GPR173 leads to neurotoxicity, we conducted in vitro whole-cell patch-clamp recordings 4 months after administering AAV. Given the significant role of excitatory neurons in the cortex, we used patch-clamp recordings to evaluate the excitability of cortical neurons from mice overexpressing GPR173. Our results revealed that the number of action potentials in GPR173-upregulated neurons was similar to that in the control group, even when subjected to currents of 400 pA (Fig. 7A and B). In addition, there was no noticeable difference in the amplitude (Fig. 7C), resting membrane potential (Fig. 7D), half-width of the action potential (AP) (Fig. 7E), or latency of the first APs (Fig. 7F) among the three groups. These findings suggest that virus-transfected excitatory neurons maintain normal functionality after the long-term expression of AAV-PHP.eB.

GPR173 activation promotes osteoblastic differentiation, whereas osteogenic differentiation is critical for bone homeostasis; an imbalance between these processes contributes to the progression of osteoporosis [23]. The findings of our behavioral study are consistent with studies demonstrating that CCK exerts significant effects on satiation and energy intake, which may play a role in weight regulation [63, 64]. Consequently, it can be hypothesized that the overexpression of GPR173 may result in body mass changes in a normal mouse model. To assess body weight changes of each mouse, we conducted a longitudinal study over 15 weeks. As depicted in Fig. 7G, the weight of the three groups of mice demonstrated a trend of continuous growth. However, the weight gain rate of the mice in the GPR173-injected group was slower ($^{*}P < 0.05$), which may be attributed to side effects of the overexpression. In Fig. 7H, we calculated the effect of virus expression on the survival rate of mice. The results revealed that apart from one mouse in the sham group that died before day 50, all other mice survived until the last perfusion. This suggests that the GPR173 overexpression does not cause fatal toxicity or pose a threat to the life of mice. Further investigations are necessary to elucidate the precise mechanisms by which GPR173 influences bone formation and its subsequent impact on body composition.

Thus, our findings provide strong evidence that enhanced GPR173 expression can effectively reduce seizure activity and alleviate epileptic episode severity in a preclinical chronic epilepsy model.

DISCUSSION

Excessive strengthening of excitatory synapses has been implicated in various neurological disorders, including epilepsy [65]. Hyperexcitability and hypersynchronous firing of neuronal ensembles at the micro- and macro-circuit levels, caused by the E/I imbalance, can trigger seizure initiation [2, 66]. Despite implementing various treatment paradigms aimed at restoring the E/I balance, success has been minimal. Previous research has

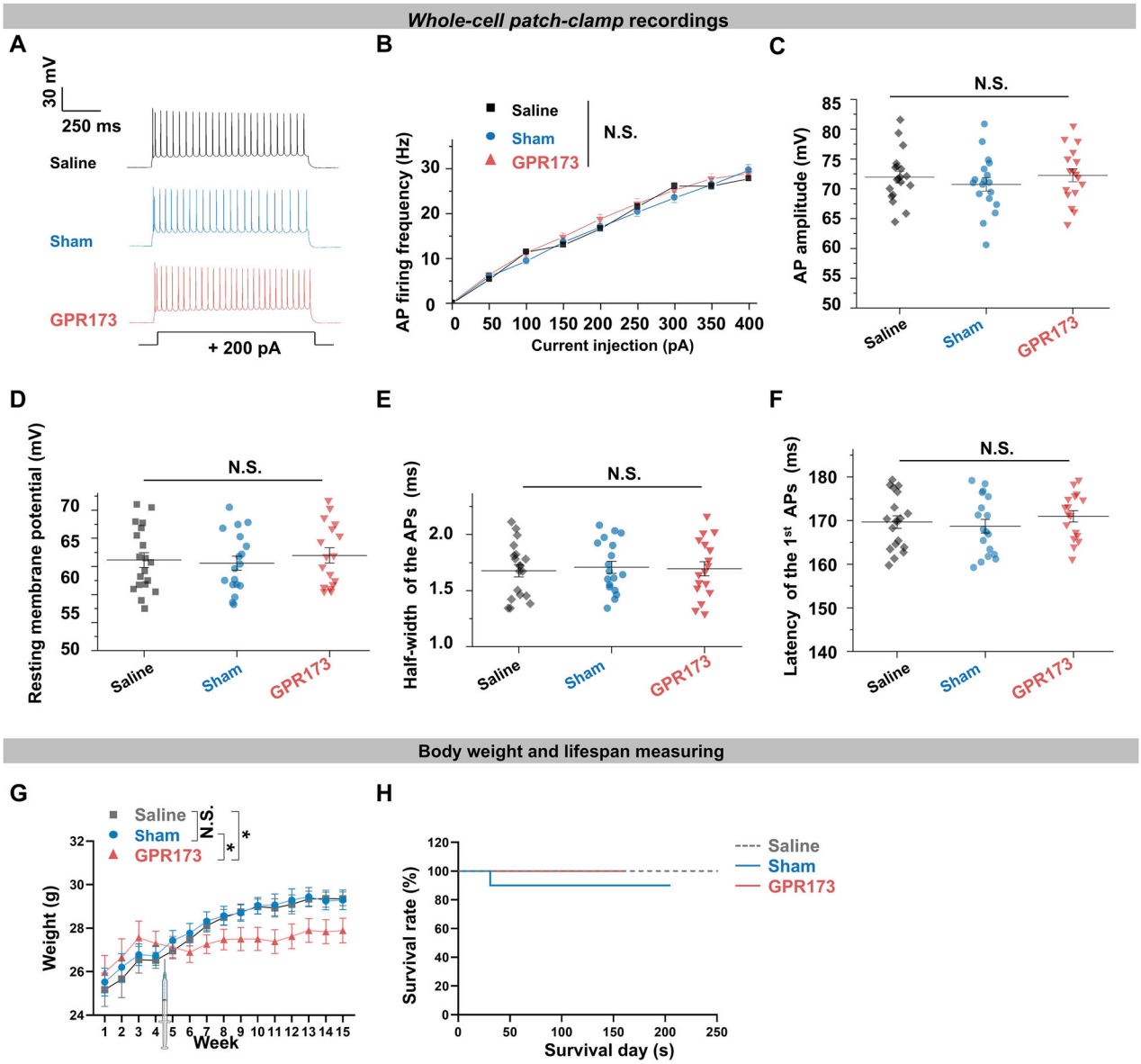

Fig. 7 AAV drives long-term GPR173 expression and does not induce abnormal firing properties in transfected excitatory neurons. **A** Examples of action potential (AP) traces evoked by current injection in cortical excitatory neurons from the mice of saline, CaMKII-Sham-mCherry, CaMKII-GPR173-mCherry groups at the age of 6 months. **B** Line chart showing the frequency of APs in excitatory neurons from the above three groups of mice (two-way ANOVA with Tukey's post hoc test, N.S.). **C** Histogram showing the amplitude of APs in response to 200 pA current injection in excitatory neurons from the three groups of mice (two-way ANOVA with Tukey's post hoc test, N.S.). **D** Histogram showing the resting membrane potential in excitatory neurons from the three groups of mice (two-way ANOVA with Tukey's post hoc test, N.S.). **E** Histogram showing half-width of the APs (two-way ANOVA with Tukey's post hoc test, N.S.). **F** Histogram showing latency of the APs (two-way ANOVA with Tukey's post hoc test, N.S.). In whole-cell patch-clamp recordings, n = 17–20 neurons per group. **G** Body weight changes of mice before and after tail vein injection (saline group, N = 9; CaMKII-Sham-mCherry group, N = 9; CaMKII-GPR173-mCherry group, N = 10; two-tailed two-sample t-test, $^*P < 0.05$; N.S.). **H** The survival rate of mice from the start of tail vein injection until the perfusion period. Deaths due to Morris water maze test were not counted (Saline group, N = 9; CaMKII-Sham-mCherry group, N = 10; CaMKII-GPR173-mCherry group, N = 8). Data are shown as mean ± standard error of the mean. AAV adeno-associated virus, N.S. not significant.

demonstrated that CCK mediates the inhibition of GABAergic synapses via a novel CCK3R (GPR173) [29], leading to the adoption of gene therapy involving exogenous upregulation of GPR173 as a new approach for treating epilepsy in this study. Following viral injection, GPR173 expression increased, and the neuronal network of the epileptic mice were gradually rebuilt to inhibit spontaneous seizures.

The formation of recurrent excitatory loops, synaptic reorganization, and network alterations, which are immense pathological changes that occur after exposure to chemoconvulsants, increase the vulnerability to seizure occurrence [67–69]. The progressive increase in spontaneous seizures over time and seizure clusters in the chronic state of seizures observed in this study are consistent with previous findings [70, 71]. These seizures were neither suppressed nor completely eradicated without therapeutic intervention. A previous study demonstrated that chronic seizures of extended duration resulted in loss of function not only in CCK neurons but also in other cell types within the hippocampus [72]. Consequently, we propose the upregulation of GPR173 in the hippocampus and cortex as a potential approach for managing chronic epilepsy. Increased expression of GPR173 in these cerebral regions may potentially restore the function of CCK neurons and

other affected cell types. This strategy could potentially ameliorate the deleterious effects of chronic seizures on hippocampal and cortical functions. Further investigation is warranted to fully elucidate the downstream mechanisms through which GPR173 upregulation influences epilepsy management and to determine its long-term efficacy in preventing neuronal loss.

Gene therapy has been proposed as a potential treatment for several brain disorders, including Parkinson's disease, Huntington's disease, and focal epilepsy [73–76]. Recent advances in gene therapy for CNS diseases have enabled targeting of specific neuron types throughout the brain using the BBB-AAV [77], thereby overcoming the limitations of targeting multiple brain areas in treating epilepsy. This progress has paved the way for exploring new therapeutic targets, with GPR173 showing promise. Our research indicates that GPR173 can significantly reduce the frequency of recurrent seizures in mouse models of chronic epilepsy without causing significant neuronal excitotoxicity. Moreover, its enhancement appeared to exert more potent anticonvulsant effects during the later stages of the disease, suggesting that this therapeutic strategy may hold significant promise for addressing persistent, treatment-refractory epilepsy. Future studies should explore the potential benefits of combining GPR173 targeting with other anticonvulsant drugs to further enhance its therapeutic efficacy and improve seizure control in patients with treatment-refractory epilepsy.

A significant limitation of epilepsy treatment, particularly the utilization of AEDs, is the manifestation of adverse and intolerable side effects in patients with epilepsy, including cognitive and motor effects [57–59]. In contrast, our treatment did not appear to induce any noticeable impairments in locomotion or spatial memory, even after long-term GPR173 upregulation. Notably, the overexpression of GPR173 in excitatory neurons may contribute to maintaining the mice's energy levels, as their total distance after virus injection remained constant in the OFT. The only minor side effect observed so far is the effect on body weight, which is prevalent in numerous drug treatments. This outcome aligns with studies indicating that CCK exerts substantial effects on satiation and energy intake and may be involved in weight regulation [63, 64]. Furthermore, this effect may also be closely associated with GPR173, as GPR173 has been reported to influence metabolic pathways, bone formation, and homeostasis [22–24]. These findings warrant further research. Although we were unable to examine all potential side effects of our therapy, other possible consequences of GPR173 overexpression that were not assessed in this study may necessitate further evaluation before clinical trials. The potential effect of GPR173 overexpression on metabolic pathways and energy regulation highlights the need for comprehensive metabolic profiling in future studies. Additionally, investigating the effects of GPR173 upregulation on other physiological systems, such as cardiovascular and endocrine systems, would provide a more complete understanding of its safety profile. Long-term follow-up studies in animal models are also crucial to assess any delayed or cumulative effects of sustained GPR173 overexpression on overall health and lifespan.

In this study, we demonstrated that CCK3R (GPR173) could be a more promising target for drug development than GABA receptors because it mediates the enhancement of GABAergic action rather than direct GABAergic inhibition. Our successful gene therapy for chronic seizures further supports the concept of enhancing inhibition through CCK3R and presents a novel, more effective approach for treating epilepsy. Although we were unable to completely suppress seizures with AAV vectors overexpressing GPR173, we improved treatment efficacy by modifying the promoter, which increased the expression efficiency of BBB-penetrating AAV and delivered the target protein to specific neuron types and brain regions. Increased dosage or multiple applications of GPR173 vectors may lead to total suppression of seizures. Furthermore, identifying specific agonists for GPR173 or its downstream pathways may be a promising strategy for treating chronic seizures. Gene therapy approaches have several appealing characteristics, including the long-term expression of therapeutic genes, advances in promoter technology for controlling transgene expression from viral vectors, and the ability of viral vectors to achieve more precise targeting. In summary, gene therapy is a promising treatment strategy for addressing deficiencies in pharmacological manipulation.

MATERIALS AND METHODS

Ethics and participants

This study received ethical approval from the Animal Research Ethics Sub-Committee of the City University of Hong Kong (Kowloon, Hong Kong), under reference # A0438 & AN-STA-00000326. All study design and experimental methods adhered strictly to the relevant institutional guidelines and regulations. No human materials were involved in this research.

Animals

All procedures were carried out following guidelines approved by the Animal Research Ethics Sub-Committee of the City University of Hong Kong. The following transgenic mice were utilized: CCK-ires-Cre ($Cck^{tm1.1(Cre)Zjh}$/J, C57BL/6 J background, hereafter referred to as CCK-Cre; the Jackson Laboratory, Barport, Maine, US), and C57BL/6 J mice.

Intrahippocampal KA injection-induced chronic seizure model establishment

Surgery. We anesthetized male C57BL/6 J mice (aged 6–7 weeks) with pentobarbital (100 mg/kg) and performed a craniotomy perpendicularly to the CA1 region of the hippocampus (−2.06 mm posterior to the bregma, −1.80 mm to the midline, and −1.60 mm to the dura), and then we injected 650 nL KA (0.3 mg/mL) at a speed of 30 nL/min. After recovering from anesthesia, we observed the mice for at least 1 h for signs of acute epileptic seizures before placing them back into their cages for routine monitoring. Mice injected with KA alone (Fig. 1) were monitored for 16 weeks after the injection.

Observation and assessment of epilepsy via MMRS. Mice were individually housed under standard 12-h light/dark cycles and stable temperatures (23–25 °C) with unrestricted access to food and water. These mice were closely monitored and recorded for at least 3 weeks post-surgery using a 360° smart camera, which operated 24 h a day.

To achieve automatic epileptic ictal recognition, we developed a software program based on a open-source deep learning architecture (utilizing Pytorch and Python development environments). This software program consists of four main components (Fig. 1B): video extraction, frame tabbing, movement prediction, and seizure confirmation through manual checking. To enhance the video frame contrast, histogram equalization was applied by equalizing different grayscale pixels in the gray frames. The differences between the previous, current, and next frames were computed, and a threshold value of k was used to detect the noise in the difference. If the difference in the same pixel of the two frames was less than k, it was treated as noise and reduced to 0 (grayscale value). Otherwise, the difference was enhanced to 255 (grayscale value). The summation of each pixel value for the difference was used to determine whether the animal had moved between the three frames. If the animal had not moved, the video interval between frames was deleted. Consequently, some parts of the video were removed when the animal was asleep or inactive.

The evaluation of the seizures was conducted blindly, with the examiners of the video footage being unaware of the mice's history. The severity of seizures was assessed using a revised Racine scale, which was divided into five stages: 1) mouth and facial movements, 2) head nodding, 3) forelimb clonus, 4) rearing, and 5) rearing and falling. For our 24-h behavioral monitoring and analysis, we focused on stages 3–5 in our current study (see Supplementary videos 1–3, Table S1).

Surgery and virus injections

The animals were anesthetized using pentobarbital (100 mg/kg) supplemented with atropine (0.05 mg/kg). The anesthetized mice were then immobilized using a stereotaxic device (RWD Life Sciences). Subsequently,

craniotomy was performed to access the auditory cortex, and the dura mater was opened (AC, located at −2.0 to −3.0 mm posterior to the bregma and −4.0 to −4.3 mm lateral to the midline).

Researchers have designed a BBB-penetrating AAV-PHP.eB, produced by BrainVTA (Wuhan, China). AAV included a woodchuck hepatitis virus post-transcriptional regulatory element (WPRE) and expressed either an enhanced green fluorescent protein (eGFP) or orphan GPR173 under the control of the neuron-specific enhancer sequence CMV (rAAV-CMV-GPR173-eGFP-PHP.eB or rAAV-CMV-Sham-eGFP-PHP.eB), or a red fluorescent protein (mCherry) and modified CaMKII under the same regulatory element (rAAV-CaMKII-Sham-mCherry-PHP.eB).

A cocktail of rAAV-mDlx-DIO-ChR2-mCherry-WPRE-pA (2.09 E + 12 vg/mL; BrainVTA) and rAAV-CMV-GPR173-eGFP-PHP.eB (1.01 E + 12 vg/mL) was injected into the cortex of CCK-Cre mice (Fig. 2). Four auditory cortex (AC) locations were injected with 300 nL of the AAV vector at a rate of 30 nL/min per site and 0.65 mm depth under the dura (Nanoliter Injector, World Precision Instruments).

Whole-cell current and voltage-clamp recordings

Briefly, fully anesthetized mice received transcardial perfusion with NMDG-aCSF (92 mM NMDG, 2.5 mM KCl, 1.2 mM NaH_2PO4, 30 mM $NaHCO_3$, 20 mM HEPES, 25 mM glucose, 2 mM thiourea, 5 mM Na-ascorbate, 3 mM Na-pyruvate, 0.5 mM $CaCl_2{\cdot}4H_2O$, and 10 mM $MgSO_4{\cdot}7H_2O$; pH adjusted to 7.3–7.4 with concentrated HCl). The brain was gently and rapidly extracted from the skull and then cut into 300 μm-thick sections with a vibratome (Leica VT1200S). Slices were transferred into NMDG-aCSF for 10 min at 32–34 °C to allow protective recovery and then transferred to HEPES-aCSF (92 mM NaCl, 2.5 mM KCl, 1.2 mM NaH_2PO_4, 30 mM $NaHCO_3$, 20 mM HEPES, 25 mM glucose, 2 mM thiourea, 5 mM Na-ascorbate, 3 mM Na-pyruvate, 2 mM $CaCl_2{\cdot}4H_2O$, and 2 mM $MgSO_4{\cdot}7H_2O$; pH adjusted to 7.3–7.4) at 25 °C for at least 1 h before recording.

Brain slices were then bathed in room-temperature recording aCSF (124 mM NaCl, 2.5 mM KCl, 1.2 mM NaH_2PO_4, 24 mM $NaHCO_3$, 5 mM HEPES, 12.5 mM glucose, 2 mM $CaCl_2{\cdot}4H_2O$, and 2 mM $MgSO_4{\cdot}7H_2O$, ~25 °C). Whole-cell recordings were made at the auditory cortex using a Multiclamp 700B amplifier and Digital 1440 A digitizer. Patch pipettes with 5–7 MΩ resistance were pulled from borosilicate glass (WPI) with a Sutter-87 puller (Sutter). The internal solution contained: 130 mM K-Gluconate, 10 mM NaCl, 10 mM HEPES, 1 mM EGTA, 3 mM Mg-ATP, 2 mM Na-GTP, and 0.133 mM $CaCl_2$; pH adjusted to 7.3 with 1 M KOH; 290–300 mOsm. Similarly, recordings were made after the Giga-Ohm seal formation, holding at −65 to −60 mV and terminated if Rs changed more than 20%. We selected pyramidal neurons based on the $eGFP^+$ pyramidal-like shape and the firing pattern of regular spiking by injecting step currents.

We applied laser stimulation through an optical fiber placed approximately 200 μm from the recording neuron using the Aurora-220 (473 nm, NEWDOON, China) to activate $ChR2^+$ neurons (GABAergic). We recruited neurons that responded only to the laser pulse in our experiment. We delivered high-frequency laser stimulation (HFLS; 10-pulse burst at 40 Hz, repeated for 10 trials) or LFLS (1 Hz, 100 pulses) with a 15-s interval. We recorded IPSCs in response to the laser stimulation (1 pulse per 15 s, 5 ms in duration) under voltage-clamp recording mode (holding at −60 mV to −50 mV) for 5 min as the baseline before and for 25 min after the HFLS or LFLS.

AAV-PHP.eB intravenous injection in epileptic mice

After the C57BL/6 J male mice (9–10 weeks old) showed a stable occurrence of spontaneous recurrent seizures, we randomly divided the epileptic mice into two groups (experimental and control). We recorded the daily seizure occurrences for 2 weeks as the pre-treatment baseline for each mouse. For the administration of CMV-AAV-CMV-GPR173-eGFP-PHP.eB, an intravenous intracranial injection was used. This decision was made based on several considerations. First, establishing a sufficient number of chronic epilepsy mouse models presents a notable challenge. Second, the virus intended for injections is expensive and difficult to obtain. Given the limited availability of mice with chronic epilepsy, we opted for intravenous 'administration to maximize the probability of successful viral delivery. The solution was injected under a microscope to ensure adequate viral delivery.

We anesthetized the epileptic mice with pentobarbital sodium (100 mg/kg) and atropine (0.05 mg/kg; Sigma). We opened the skull near the lambda to expose the transverse venous sinus for virus injection. The experimental group of mice received an injection of 50 μL rAAV-CMV-GPR173-eGFP-PHP.eB-WPREs (CMV-GPR173-eGFP, 5.01 E + 12 vg/mL), while the control group received rAAV-CMV-Sham-eGFP-PHP.eB-WPREs (CMV-Sham-eGFP, 5.32 E + 12 vg/mL). The PHP.eB serotype virus, which readily crosses the BBB for brain transduction, was produced using standard methods. We used a glass pipette tip (at an angle of approximately 30–45°) to touch the surface of the transverse venous sinus slowly. After the glass pipette tip penetrated the vessel, we injected a total of 50 μL of the virus at the rate of 1000 nL/min.

We monitored the mice for seizure occurrences for another 8 weeks after the CMV-GPR173-eGFP or CMV-Sham-eGFP intravenous injection.

Tail vein injection

The mice were anesthetized using a cocktail of ketamine, xylazine, and acepromazine at doses of 80–100, 8–20, and 1–3 mg/kg, respectively. They were then fixed in an auxiliary device, and their tails were placed in a ring slot. The tail was wiped with alcohol to improve blood vessel visibility, and an LED lamp was used to illuminate the tail vein. Using naked eyes, 0.05 mL rAAV-CaMKII-GPR173-mCherry-PHP.eB (CaMKII-GPR173-mCherry, 5.00 E + 12 vg/mL) or rAAV-CaMKII-Sham-mCherry-PHP.eB (CaMKII-Sham-mCherry, 2.00 E + 12 vg/mL; BrainVTA) was slowly injected into the tail blood vessels of mice. After the procedure, the mice were placed in a warm box until they awakened. This approach was followed as it offers a more efficient and less invasive method of viral delivery. Tail vein injections not only mitigated stress in mice but also enhanced the overall experimental success rate.

Spontaneous locomotion detection in mice

Our investigation involved using a self-developed program to examine animal movement. We determined each mouse's daily active time, which includes activities such as movement, dining, grooming, and exploration.

Weight monitoring

The administration of a synthetic virus can potentially result in weight gain or weight loss in mice. Therefore, weight change is considered an essential factor in evaluating the adverse effects of the virus. Due to the minimal fluctuations in mouse weight over 1 week, we utilized a weighing machine to measure the mice's weight 1–2 times a week for 15 weeks. The data are presented as the average weight of each mouse per week.

Health monitoring

The animals were closely monitored daily to ensure that they did not have any infections, exhibited extremely low levels of activity, or suffered significant physical injuries. In the event of accidental injury, carprofen (Phrl452-IG; Sigma-Aldrich China, Inc.) was administered. In more severe cases, such as when mice experience severe complications, uncontrollable seizures following surgery, or obvious distress, an overdose of pentobarbital sodium was administered to euthanize them.

OFT

A container measuring 50 cm × 50 cm × 50 cm (hereafter referred to as OF) was prepared for the experiment and surrounded by partitions made of white plastic. The area surrounding the OF is outlined in red, while the central area is indicated by a green frame, 10 cm away from the red frame in width and length. The mice were placed in the room 1 h in advance to allow them to acclimate to the environment. Each mouse was placed in the OF for 10 min to explore the space, and the container was cleaned with 75% alcohol before each trial. The movements of each mouse were recorded using a camera, and the resulting videos were processed using Smart video tracking software 3.0 (Smart v3.0), which generated summary reports including the time spent in the central area and the total distance traveled. The OFT was conducted before and after injection of the constructed virus into the tail vein.

NORT

The three stages of habituation, training, and testing were integrated into the NORT, which employed a square structure consisting of five white acrylic panels (40 cm × 40 cm × 40 cm). Before the test, the experimenter familiarized the mice with the environment and placed them in a separate room for 1 h. In the habituation phase on day 1, each mouse was allowed to explore the arena for 10 min without any objects. On day 2, two identical objects were introduced to each mouse to facilitate familiarity, and the mice were given a 5-min exploration period. After a 24-h interval (day 3), one of the objects was replaced with a different one, and each

mouse was allowed to explore for 5 min. The camera recorded the activity, and Smart v3.0 was utilized to track the movement of the mice. Some mice were excluded from the experiment because of biased or unsuitable behavior. The duration and number of times the mouse touched the old and novel objects were counted using Smart v3.0. The preference index was calculated as (time spent exploring the novel object / total time spent exploring old and novel objects) × 100%. A novel object recognition test was conducted before and after the tail vein injection.

MWMT

Briefly, a swimming pool with a diameter of approximately 120 cm was placed in a separate room, as illustrated in Fig. 6J. Four stickers of different shapes were placed on the inner wall of the swimming pool for identification. The water was dyed white with nontoxic pigments, and the water temperature was maintained at 25 °C. In the visible platform training phase (Day 0), the platform was positioned at the midpoint between the center of the pool and the wall and marked with a flag. Each mouse was gently placed in the water from five different quadrants (S, N, S, E, and W in order), while the platform was placed correspondingly in the SW, NW, NE, Center, and SE positions. The time it took for the mouse to escape from the water and climb onto the platform was recorded. The platform was then placed at quadrant 3 for the following 7 days (Days 1–7) and was floored until the mouse could not see it, while the flag was also removed. Each mouse was placed into the water from four different quadrants respectively every day in the hidden platform training phase.

In the above two stages, if the mouse did not escape from the water within 60 s, it was pulled to the platform and allowed to stay there for 15–20 s. On the last day (day 8), the platform was removed, and each mouse was allowed to swim in the pool for 60 s while the swimming video was recorded. Heat maps of mouse trajectories and the proportion of time spent in each quadrant were analyzed via MATLAB (R2016b) software. Since the MWM test greatly impacts mice's health, we only performed this experiment after tail vein injection.

Immunohistochemical staining

For immunohistochemistry, the mice were deeply anesthetized with an overdose of pentobarbital sodium. The mice were transcardially perfused with 30 mL of cold phosphate-buffered saline (PBS) and 30 mL of 4% (w/v) paraformaldehyde (PFA). Brain tissue was removed, post-fixed with 4% PFA, and treated with 30% (w/v) sucrose in 4% PFA at 4 °C for 2–3 days. The brain tissue was sectioned on a cryostat (30–50 μm for standard staining and 10 μm for super-resolution imaging) (Leica CM3500, Germany) and preserved with antifreeze buffer (20% (v/v) glycerin and 30% (v/v) ethylene glycol diluted in PBS) at −20 °C. For immunostaining and statistical analysis of co-labeled neurons and axonal synapses in the AC, serial sections containing the AC were selected for analysis. The brain sections were rinsed three times with PBS and blocked with blocking buffer (10% (v/v) goat serum in PBS with 0.5% (v/v) Triton X-100) for 3 h at room temperature. Sections were incubated with the primary antibody (Table S2) at 4 °C for 24–36 h. After washing three times in PBS (10 min each), the sections were incubated with the corresponding fluorophore-conjugated secondary antibodies (Table S2) for 2–3 h at 25 °C. The sections were then rinsed with PBS three times before DAPI staining (1:10,000 (v/v) diluted in PBS) or mounting. All the sections were mounted on slides with 70% (v/v) glycerin in PBS.

Image acquisition and analysis

Images were taken at 10X, 20X, 60X, and 100X magnification using a Nikon A1hD25 confocal microscope (Nikon, Japan). The confocal microscope was equipped with a time-delay integration camera, and line scanning was performed, allowing for quick acquisition of high-resolution fluorescent signals. Images were captured at 20X magnification and merged using the same laser settings for the parallel study. We adjusted the gain and exposure parameters for each image to optimize the results. Z-stacks of images were captured throughout the tissue to show the labeling details for the magnified images. To quantify colocalization, we counted neurons expressing the indicated reporter by analyzing only the corresponding color channel. Among these cells, we counted the number of neurons co-expressing the marker of interest using the Nikon imaging analysis software (NIS-Elements Viewer 5.21). Bright-spot detection was performed in the brain regions of interest using appropriate fluorescent thresholds. A neuron was considered positive for a given marker if its corresponding signal was above background fluorescence. The ratio of neurons co-expressing both markers to the total number of cells expressing only the reporter was calculated. The "n" values in the figures represent the number of biological replicates, while "N" indicates the number of independent animals. At least three biological replicates were included for all quantifications in this study.

Quantifications, statistics, and reproducibility

Our analyses were conducted using a minimum of three independent biological replicates. Data collection and analysis were not blinded unless specified. Different research groups performed the quantification. We presented the group data as mean ± standard error of the mean. SPSS 25.0 (IBM, New York, US) and Excel were used to perform statistical analyses, including a two-tailed two-sample t-test, Student's unpaired t-test, Student's paired t-test, ANOVA with Tukey's post hoc test, and two-way RM ANOVA with Tukey's post hoc test. Asterisk or sharp symbols denote significant differences in all Figures ($*P < 0.05$, $**P < 0.01$, $***P < 0.001$, $****P < 0.0001$, $\#P < 0.05$, $\#\#\#P < 0.001$ and ####P < 0.0001). N.S. indicates that the difference was not significant. We used OriginPro 8.5 (OriginLab Corporation, Massachusetts, US), Inkscape 0.92.3 (Inkscape), and GraphPad Prism 8 (GraphPad Software, CA, US) to perform the graphing. The reference brain map with anatomical abbreviations is accessible on the Allen Brain Atlas website.

DATA AVAILABILITY

Data supporting the conclusions of this study are available from the corresponding author upon submission of a reasonable request.

REFERENCES

1. Fisher RS. Redefining epilepsy. Curr Opin Neurol. 2015;28:130–5.
2. Tóth K, Hofer KT, Kandrács Á, Entz L, Bagó A, Erőss L, et al. Hyperexcitability of the network contributes to synchronization processes in the human epileptic neocortex. J Physiol. 2018;596:317–42.
3. Ong M-S, Kohane IS, Cai T, Gorman MP, Mandl KD. Population-level evidence for an autoimmune etiology of epilepsy. JAMA Neurol. 2014;71:569.
4. Fattorusso A, Matricardi S, Mencaroni E, Dell'Isola GB, Di Cara G, Striano P, et al. The pharmacoresistant epilepsy: an overview on existant and new emerging therapies. Front Neurol. 2021;12:674483 https://doi.org/10.3389/fneur.2021.674483.
5. Kaur H, Kumar B, Medhi B. Antiepileptic drugs in development pipeline: a recent update. eNeurologicalSci. 2016;4:42–51.
6. Löscher W, Potschka H, Sisodiya SM, Vezzani A. Drug resistance in epilepsy: clinical impact, potential mechanisms, and new innovative treatment options. Pharmacol Rev. 2020;72:606–38.
7. Kumar SS. Hyperexcitability, interneurons, and loss of GABAergic synapses in entorhinal cortex in a model of temporal lobe epilepsy. J Neurosci. 2006;26:4613–23.
8. Madsen KK, White HS, Schousboe A. Neuronal and non-neuronal GABA transporters as targets for antiepileptic drugs. Pharmacol Ther. 2010;125:394–401.
9. Tang X, Jaenisch R, Sur M. The role of GABAergic signalling in neurodevelopmental disorders. Nat Rev Neurosci. 2021;22:290–307.
10. Whiting PJ. GABA-A receptor subtypes in the brain: a paradigm for CNS drug discovery?. Drug Discov Today. 2003;8:445–50.
11. Riss J, Cloyd J, Gates J, Collins S. Benzodiazepines in epilepsy: pharmacology and pharmacokinetics. Acta Neurol Scand. 2008;118:69–86.
12. Fritschy J, Paysan J, Enna A, Mohler H. Switch in the expression of rat GABAA-receptor subtypes during postnatal development: an immunohistochemical study. J Neurosci. 1994;14:5302–24.
13. Cattaneo S, Verlengia G, Marino P, Simonato M, Bettegazzi B. NPY and Gene Therapy for Epilepsy: How, When,… and Y. Front Mol Neurosci. 2021;13:608001 https://doi.org/10.3389/fnmol.2020.608001.
14. Zhang L, Wang Y. Gene therapy in epilepsy. Biomed Pharmacother. 2021;143:112075.
15. Chen W, Hu Y, Ju D. Gene therapy for neurodegenerative disorders: advances, insights and prospects. Acta Pharm Sin B. 2020;10:1347–59.
16. Weinberg MS, Samulski RJ, McCown TJ. Adeno-associated virus (AAV) gene therapy for neurological disease. Neuropharmacology. 2013;69:82–88.
17. Byun S, Lee M, Kim M. Gene therapy for Huntington's disease: the final strategy for a cure?. J Mov Disord. 2022;15:15–20.
18. Combs B, Kneynsberg A, Kanaan NM. Gene therapy models of Alzheimer's disease and other dementias. Methods Mol Biol. 2016;1382:339–66.
19. Van Laar AD, Van Laar VS, San Sebastian W, Merola A, Elder JB, Lonser RR, et al. An update on gene therapy approaches for parkinson's disease: restoration of dopaminergic function. J Parkinsons Dis. 2021;11:S173–S182.

20. Matsumoto M, Beltaifa S, Weickert CS, Herman MM, Hyde TM, Saunders RC, et al. A conserved mRNA expression profile of SREB2 (GPR85) in adult human, monkey, and rat forebrain. Mol Brain Res. 2005;138:58–69.
21. Treen AK, Luo V, Belsham DD. Phoenixin activates immortalized GnRH and kisspeptin neurons through the novel receptor GPR173. Mol Endocrinol. 2016;30:872–88.
22. McIlwraith EK, Loganathan N, Belsham DD. Regulation of Gpr173 expression, a putative phoenixin receptor, by saturated fatty acid palmitate and endocrine-disrupting chemical bisphenol A through a p38-mediated mechanism in immortalized hypothalamic neurons. Mol Cell Endocrinol. 2019;485:54–60.
23. Gu Z, Xie D, Ding R, Huang C, Qiu Y. GPR173 agonist phoenixin 20 promotes osteoblastic differentiation of MC3T3-E1 cells. Aging. 2021;13:4976–85.
24. Sun G, Ren Q, Bai L, Zhang L. Phoenixin-20 suppresses lipopolysaccharide-induced inflammation in dental pulp cells. Chem Biol Interact. 2020;318:108971.
25. Gaiarsa JL, Caillard O, Ben-Ari Y. Long-term plasticity at GABAergic and glycinergic synapses: mechanisms and functional significance. Trends Neurosci. 2002;25:564–70.
26. Castillo PE, Chiu CQ, Carroll RC. Long-term plasticity at inhibitory synapses. Curr Opin Neurobiol. 2011;21:328–38.
27. Xue M, Atallah BV, Scanziani M. Equalizing excitation-inhibition ratios across visual cortical neurons. Nature. 2014;511:596–600.
28. He K, Huertas M, Hong SZ, Tie X, Hell JW, Shouval H, et al. Distinct eligibility traces for LTP and LTD in cortical synapses. Neuron. 2015;88:528–38.
29. He L, Shi H, Zhang G, Peng Y, Ghosh A, Zhang M, et al. A Novel CCK receptor GPR173 mediates potentiation of GABAergic inhibition. J Neurosci. 2023;43:2305–25.
30. Beaulieu C. Numerical data on neocortical neurons in adult rat, with special reference to the GABA population. Brain Res. 1993;609:284–92.
31. Liu B, Li P, Sun YJ, Li Y, Zhang LI, Tao HW. Intervening inhibition underlies simple-cell receptive field structure in visual cortex. Nat Neurosci. 2010;13:89–96.
32. Sun YJ, Wu GK, Liu BH, Li P, Zhou M, Xiao Z, et al. Fine-tuning of pre-balanced excitation and inhibition during auditory cortical development. Nature. 2010;465:927–31.
33. Staley K. Molecular mechanisms of epilepsy. Nat Neurosci. 2015;18:367–72.
34. Kambli L, Bhatt LK, Oza M, Prabhavalkar K. Novel therapeutic targets for epilepsy intervention. Seizure. 2017;51:27–34.
35. Wickham J, Ledri M, Bengzon J, Jespersen B, Pinborg LH, Englund E, et al. Inhibition of epileptiform activity by neuropeptide Y in brain tissue from drug-resistant temporal lobe epilepsy patients. Sci Rep. 2019;9:1–11.
36. Kwan P, Brodie MJ. Early identification of refractory epilepsy. N Engl J Med. 2000;342:314–9.
37. Petrini EM, Ravasenga T, Hausrat TJ, Iurilli G, Olcese U, Racine V, et al. Synaptic recruitment of gephyrin regulates surface GABAA receptor dynamics for the expression of inhibitory LTP. Nat Commun. 2014;5:3921.
38. Chiu CQ, Martenson JS, Yamazaki M, Natsume R, Sakimura K, Tomita S, et al. Input-specific NMDAR-dependent potentiation of dendritic GABAergic inhibition. Neuron. 2018;97:368–77.e3.
39. He Q, Duguid I, Clark B, Panzanelli P, Patel B, Thomas P, et al. Interneuron- and GABAA receptor-specific inhibitory synaptic plasticity in cerebellar Purkinje cells. Nat Commun. 2015;6:7364.
40. Udakis M, Pedrosa V, Chamberlain SEL, Clopath C, Mellor JR. Interneuron-specific plasticity at parvalbumin and somatostatin inhibitory synapses onto CA1 pyramidal neurons shapes hippocampal output. Nat Commun. 2020;11:4395.
41. Perucca E, Bialer M, White HS. New GABA-Targeting therapies for the treatment of seizures and epilepsy: I. role of GABA as a modulator of seizure activity and recently approved medications acting on the GABA system. CNS Drugs. 2023;37:755–79.
42. Sloviter RS. The neurobiology of temporal lobe epilepsy: too much information, not enough knowledge. C R Biol. 2005;328:143–53.
43. Bello ST, Xu S, Li X, Ren J, Jendrichovsky P, Jiang F, et al. Visually or auditorily induced seizures involve the activation of nonhippocampal brain areas and hippocampal removal does not alleviate seizures in a mouse model of temporal lobe epilepsy. Epilepsia. 2024;65:218–37.
44. Hökfelt T. Neuropeptides in perspective: the last ten years. Neuron. 1991;7:867–79.
45. Gröticke I, Hoffmann K, Löscher W. Behavioral alterations in a mouse model of temporal lobe epilepsy induced by intrahippocampal injection of kainate. Exp Neurol. 2008;213:71–83.
46. Bielefeld P, Sierra A, Encinas JM, Maletic-Savatic M, Anderson A, Fitzsimons CP. A standardized protocol for stereotaxic intrahippocampal administration of kainic acid combined with electroencephalographic seizure monitoring in mice. Front Neurosci. 2017;11:1–9.
47. Rusina E, Bernard C, Williamson A. The kainic acid models of temporal lobe epilepsy. eNeuro. 2021;8:ENEURO.0337-20.2021.
48. Lüttjohann A, Fabene PF, van Luijtelaar G. A revised Racine's scale for PTZ-induced seizures in rats. Physiol Behav. 2009;98:579–86.
49. Sohal VS, Rubenstein JLR. Excitation-inhibition balance as a framework for investigating mechanisms in neuropsychiatric disorders. Mol Psychiatry. 2019;24:1248–57.
50. Canitano R, Pallagrosi M. Autism spectrum disorders and Schizophrenia spectrum disorders: excitation/inhibition imbalance and developmental trajectories. Front Psychiatry. 2017;8:1–7.
51. Wiechert P, Herbst A. Provocation of cerebral seizures by derangement of the natural balance between glutamic acid and gamma-aminobutyric acid. J Neurochem. 1966;13:59–64.
52. Fitzsimons HL, Bland RJ, During MJ. Promoters and regulatory elements that improve adeno-associated virus transgene expression in the brain. Methods. 2002;28:227–36.
53. Krook-Magnuson E, Armstrong C, Oijala M, Soltesz I. On-demand optogenetic control of spontaneous seizures in temporal lobe epilepsy. Nat Commun. 2013;4:1376.
54. Kokaia M, Andersson M, Ledri M. An optogenetic approach in epilepsy. Neuropharmacology. 2013;69:89–95.
55. Gruber B, Greber S, Sperk G. Kainic acid seizures cause enhanced expression of cholecystokinin-octapeptide in the cortex and hippocampus of the rat. Synapse. 1993;15:221–8.
56. Zhang L-X, Smith MA, Kim S-Y, Rosen JB, Weiss SRB, Post RM. Changes in cholecystokinin mRNA expression after amygdala kindled seizures: an in situ hybridization study. Mol Brain Res. 1996;35:278–84.
57. Cramer JA, Mintzer S, Wheless J, Mattson RH. Adverse effects of antiepileptic drugs: a brief overview of important issues. Expert Rev Neurother. 2010;10:885–91.
58. Mutanana N, Tsvere M, Chiweshe MK. General side effects and challenges associated with anti-epilepsy medication: a review of related literature. Afr J Prim Health Care Fam Med. 2020;12:e1–e5.
59. Zaccara G, Cincotta M, Borgheresi A, Balestrieri F. Adverse motor effects induced by antiepileptic drugs. Epileptic Disord. 2004;6:153–68.
60. Vorhees CV, Williams MT. Morris water maze: procedures for assessing spatial and related forms of learning and memory. Nat Protoc. 2006;1:848–58.
61. Scharfman HE. The neurobiology of epilepsy. Curr Neurol Neurosci Rep. 2007;7:348–54.
62. Cossart R, Bernard C, Ben-Ari Y. Multiple facets of GABAergic neurons and synapses: multiple fates of GABA signalling in epilepsies. Trends Neurosci. 2005;28:108–15.
63. Warrilow A, Turner M, Naumovski N, Somerset S. Role of cholecystokinin in satiation: a systematic review and meta-analysis. Br J Nutr. 2023;129:2182–90.
64. Little TJ, Horowitz M, Feinle-Bisset C. Role of cholecystokinin in appetite control and body weight regulation. Obes Rev. 2005;6:297–306.
65. Abegg MH, Savic N, Ehrengruber MU, McKinney RA, Gähwiler BH. Epileptiform activity in rat hippocampus strengthens excitatory synapses. J Physiol. 2004;554:439–48.
66. Jiruska P, de Curtis M, Jefferys JGR, Schevon CA, Schiff SJ, Schindler K. Synchronization and desynchronization in epilepsy: controversies and hypotheses. J Physiol. 2013;591:787–97.
67. Ben-Ari Y, Dudek FE. Primary and secondary mechanisms of epileptogenesis in the temporal lobe: there is a before and an after. Epilepsy Curr. 2010;10:118–25.
68. Cavazos JE, Cross DJ. The role of synaptic reorganization in mesial temporal lobe epilepsy. Epilepsy Behav. 2006;8:483–93.
69. Royer J, Bernhardt BC, Larivière S, Gleichgerrcht E, Vorderwülbecke BJ, Vulliémoz S, et al. Epilepsy and brain network hubs. Epilepsia. 2022;63:537–50.
70. Lisgaras CP, Scharfman HE. Robust chronic convulsive seizures, high frequency oscillations, and human seizure onset patterns in an intrahippocampal kainic acid model in mice. Neurobiol Dis. 2022;166:105637.
71. Upadhya D, Kodali M, Gitai D, Castro OW, Zanirati G, Upadhya R, et al. A model of chronic temporal lobe epilepsy presenting constantly rhythmic and robust spontaneous seizures, co-morbidities and hippocampal neuropathology. Aging Dis. 2019;10:915.
72. Franz J, Barheier N, Wilms H, Tulke S, Haas CA, Häussler U. Differential vulnerability of neuronal subpopulations of the subiculum in a mouse model for mesial temporal lobe epilepsy. Front Cell Neurosci. 2023;17:1142507 https://doi.org/10.3389/fncel.2023.1142507.
73. LeWitt PA, Rezai AR, Leehey MA, Ojemann SG, Flaherty AW, Eskandar EN, et al. AAV2-GAD gene therapy for advanced Parkinson's disease: a double-blind, sham-surgery controlled, randomised trial. Lancet Neurol. 2011;10:309–19.
74. Lieb A, Qiu Y, Dixon CL, Heller JP, Walker MC, Schorge S, et al. Biochemical autoregulatory gene therapy for focal epilepsy. Nat Med. 2018;24:1324–9.
75. Wu Z, Parry M, Hou X-Y, Liu M-H, Wang H, Cain R, et al. Gene therapy conversion of striatal astrocytes into GABAergic neurons in mouse models of Huntington's disease. Nat Commun. 2020;11:1105.

76. Wykes RC, Heeroma JH, Mantoan L, Zheng K, MacDonald DC, Deisseroth K, et al. Optogenetic and potassium channel gene therapy in a rodent model of focal neocortical epilepsy. Sci Transl Med. 2012;4:161ra152.
77. Hudry E, Vandenberghe LH. Therapeutic AAV gene transfer to the nervous system: a clinical reality. Neuron. 2019;101:839–62.

ACKNOWLEDGEMENTS

We thank the following charitable foundations for their generous support to J.H: Wong Chun Hong Endowed Chair Professorship, Charlie Lee Charitable Foundation, and Fong Shu Fook Tong Foundation. We acknowledge the Open Access Publishing Fund of the City University of Hong Kong for partially supporting the open access publication of this work.

AUTHOR CONTRIBUTIONS

LH, YJY, and JFH designed the experiments. LH, LYZ, and JFH wrote the paper. LH designed the viral vectors and conducted the virus injection.LH, DXZ, and XY conducted brain-slice experiments. YJY, LYZ, FXJ, and LH conducted the intrahippocampal KA injection and intravenous virus, tail vein delivery experiments. YJY, YDZ, and LYZ performed the camera settings and epilepsy assessment. JMR and ZJX worked for the mice's seizure recognition system (MMRS). YJY, LYZ, and FXJ helped in the manual checking of the seizures. LYZ, FXJ, YDZ, and YYS conducted behavioral tests. LH and LYZ performed staining and imaging with the help of FXJ, YDZ, and YYS.

FUNDING

This work was supported by funding from the following: Hong Kong Research Grants Council, General Research Fund: CityUHK 11103922, CityUHK 11104923, CityUHK 11104524. Hong Kong Research Grants Council, Collaborative Research Fund: C1002-24W, C5053-22G. Hong Kong Research Grants Council, Senior Research Fellow Scheme: SRFS2324-1S02. Hong Kong Health Bureau, Health and Medical Research Fund: 09203656. Innovation Technology Commission of the Hong Kong SAR, China: Health@InnoHK program.

COMPETING INTERESTS

The authors declare no competing interests.

ADDITIONAL INFORMATION

Supplementary information The online version contains supplementary material available at https://doi.org/10.1038/s41398-025-03680-1.

Correspondence and requests for materials should be addressed to Ling He or Jufang He.